The Plant Cell, Vol. 25: 2115–2131, June 2013, www.plantcell.org © 2013 American Society of Plant Biologists. All rights reserved.

SALT-RESPONSIVE ERF1 Regulates Reactive Oxygen Species–Dependent Signaling during the Initial Response to Salt Stress in Rice[W]

Romy Schmidt,[a,b] Delphine Mieulet,[c] Hans-Michael Hubberten,[b] Toshihiro Obata,[b] Rainer Hoefgen,[b] Alisdair R. Fernie,[b] Joachim Fisahn,[b] Blanca San Segundo,[d] Emmanuel Guiderdoni,[c] Jos H.M. Schippers,[a,b,1] and Bernd Mueller-Roeber[a,b]

[a] Institute of Biochemistry and Biology, University of Potsdam, 14476 Potsdam, Germany
[b] Max Planck Institute of Molecular Plant Physiology, 14476 Potsdam, Germany
[c] Centre de Coopération Internationale en Recherche Agronomique pour le Développement, Unité Mixte de Recherche, Genetic Improvement and Adaptation of Mediterranean and Tropical Plants, 34398 Montpellier, cedex 5, France
[d] Department of Molecular Genetics, Centre for Research in Agricultural Genomics, Consejo Superior de Investigaciones Científicos, Institute of Agro-food Research and Technology, Autonomus University of Barcelona, University of Barcelona, Bellaterra (Cerdanyola del Vallés), 08193 Barcelona, Spain

ORCID ID: 0000-0002-1410-464X (B.M-R.).

Early detection of salt stress is vital for plant survival and growth. Still, the molecular processes controlling early salt stress perception and signaling are not fully understood. Here, we identified *SALT-RESPONSIVE ERF1* (*SERF1*), a rice (*Oryza sativa*) transcription factor (TF) gene that shows a root-specific induction upon salt and hydrogen peroxide (H_2O_2) treatment. Loss of *SERF1* impairs the salt-inducible expression of genes encoding members of a mitogen-activated protein kinase (MAPK) cascade and salt tolerance–mediating TFs. Furthermore, we show that SERF1-dependent genes are H_2O_2 responsive and demonstrate that SERF1 binds to the promoters of *MAPK KINASE KINASE6* (*MAP3K6*), *MAPK5*, *DEHYDRATION-RESPONSIVE ELEMENT BINDING2A* (*DREB2A*), and *ZINC FINGER PROTEIN179* (*ZFP179*) in vitro and in vivo. SERF1 also directly induces its own gene expression. In addition, SERF1 is a phosphorylation target of MAPK5, resulting in enhanced transcriptional activity of SERF1 toward its direct target genes. In agreement, plants deficient for *SERF1* are more sensitive to salt stress compared with the wild type, while constitutive overexpression of *SERF1* improves salinity tolerance. We propose that SERF1 amplifies the reactive oxygen species–activated MAPK cascade signal during the initial phase of salt stress and translates the salt-induced signal into an appropriate expressional response resulting in salt tolerance.

INTRODUCTION

Saline soil water constrains plant growth by an osmotic and/or toxic effect of Na^+ within the plant (Munns, 2005). Therefore, sensing of salt and dehydration stresses is of utmost importance in the process of achieving cellular homeostasis in plants (Conde et al., 2011). The appropriate adaptation response is dictated via the regulation of genes in cells and tissues that alter plant metabolism and growth (Mochida and Shinozaki, 2010). In particular, dehydration due to high salinity or drought stress triggers the biosynthesis of the phytohormone abscisic acid (ABA). Subsequently, ABA induces the expression of a significant set of genes to adapt plant growth under drought and saline conditions (Boudsocq and Laurière, 2005). Furthermore, salt stress increases the level of reactive oxygen species (ROS) like hydrogen peroxide (H_2O_2) and superoxide anion (Bienert et al., 2006; Hong et al., 2009). Although toxic by nature, ROS have now been recognized as vital signaling components in many biological processes (Mittler et al., 2011; Schippers et al., 2012). Salt-induced ROS are predominantly represented by H_2O_2 , both outside and inside the cell (Yang et al., 2007; Pang and Wang, 2008). Extracellular ROS production depends on the activity of NADPH oxidases that contribute to salt stress tolerance in *Arabidopsis thaliana* (Ma et al., 2012). In rice (*Oryza sativa*), NADPH oxidase–dependent H_2O_2 production emerges within several minutes of salt stress (Hong et al., 2009). Thus, ROS production initiates an early adaptational signal cascade to unfavorable ionic root environments. Similarly, the early response regulatory network triggered by oxidative signals is of great importance for the adaptation of rice to cold stress (Cheng et al., 2007). Moreover, genes responding to oxidative stress are activated earlier than those mediated by ABA (Yun et al., 2010).

It is currently unknown how the H_2O_2 signal is perceived. However, a signal transduction cascade has been proposed in which a mitogen-activated protein kinase (MAPK) cascade and downstream transcription factors (TFs) represent key regulatory components of ROS signaling (Skopelitis et al., 2006; Pang and Wang, 2008). Activation of the MAPK signaling pathway can result in induction or activation of different TFs that promote the expression of ROS-producing and ROS-scavenging enzymes (Mittler et al., 2004). Several members of the rice MAPK pathway

[1] Address correspondence to schippers@mpimp-golm.mpg.de.
The author responsible for distribution of materials integral to the findings presented in this article in accordance with the policy described in the Instructions for Authors (www.plantcell.org) is: Jos H.M. Schippers (schippers@mpimp-golm.mpg.de).
[W] Online version contains Web-only data.
www.plantcell.org/cgi/doi/10.1105/tpc.113.113068

are encoded by abiotic stress-responsive genes (Jung et al., 2010). In rice, the MAPK kinase kinase (MAP3K)–encoding gene *DROUGHT-HYPERSENSITIVE MUTANT1* confers drought stress tolerance by regulating ROS scavenging (Ning et al., 2010). Likewise, *MAPK5* confers enhanced tolerance to salt and osmotic stress when overexpressed (Xiong and Yang, 2003). In *Arabidopsis*, a MAPK module consisting of MEKK1-MKK2-MPK4/MPK6 was found to regulate salt tolerance (Nakagami et al., 2005). Moreover, the *mkk2* mutant exhibits a salt-sensitive phenotype (Teige et al., 2004). A downstream target of MPK6 is the Na^+/H^+ antiporter Salt Overly Sensitive1 (SOS1), a major regulator of ion homeostasis under salt stress (Shi et al., 1999; Yu et al., 2010). Furthermore, deregulated expression of MAPK genes alters the expression of salt stress–related TFs (Kishi-Kaboshi et al., 2010; Kong et al., 2011). In addition, targets of MAPK proteins are mainly TFs (Popescu et al., 2009), underlining the direct connection with the MAPK signal cascade. The expression of many TF genes, including members of the HSF, WRKY, C_2H_2 zinc-finger, bZIP, MYB, and AP2/ERF families, has been shown to be H_2O_2 induced (Miao et al., 2004; Nishizawa et al., 2006; Davletova et al., 2005; Sun et al., 2010; Yun et al., 2010). Several zinc-finger proteins (ZFPs) contribute to salt tolerance by modulating oxidative stress responses. For example, overexpression of *ZFP179* in rice improves salt tolerance accompanied by an enhanced oxidative stress tolerance (Sun et al., 2010). Besides ZFPs, members of, for example, the AP2/ERF, MYB, WRKY, and NAC families regulate salt tolerance in rice. Enhanced expression of *DEHYDRATION-RESPONSIVE ELEMENT BINDING2A* (*DREB2A*) results in improved dehydration and salt stress tolerance in rice (Mallikarjuna et al., 2011). Additionally, three rice NAC TFs (i.e., *STRESS-RESPONSIVE NAC1* [SNAC1], SNAC2, and NAC5) act as positive regulators of the salt stress response (Hu et al., 2006, 2008; Takasaki et al., 2010).

Here, we characterized the salt- and H_2O_2-responsive TF gene *SERF1* and demonstrated that it has a critical role for the salt stress response of rice. By establishing knockout, knockdown, and overexpression lines, we show that SERF1 is a positive regulator of salt tolerance by regulating the expression of a salt-responsive MAPK cascade and well established salt tolerance–mediating TF genes. Furthermore, MAPK5 interacts with SERF1, thereby enhancing its transcriptional activity toward its target genes. Based on our analysis, we present a model of an H_2O_2-mediated molecular signaling cascade important for the initial response to salinity in rice in which SERF1 functions as a central hub.

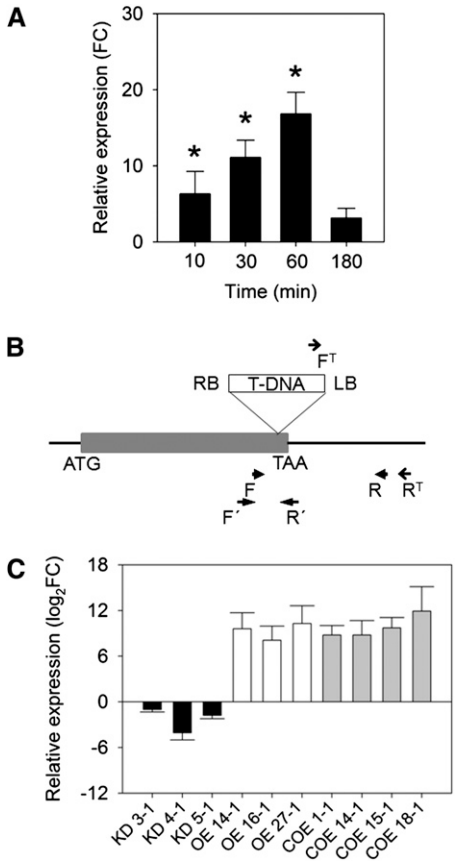

Figure 1. Identification of *SERF1* and Isolation of Transgenic Lines.

(A) Relative root mRNA levels of *SERF1* following stress treatment. Four-week-old wild-type plants were treated with 100 mM NaCl for 10, 30, 60, or 180 min. Data represent means ± SE from three independent biological replicates, and an asterisk indicates a significant difference between treated and control samples harvested at the same time points ($P \leq 0.05$). FC, fold increase over controls.

(B) Insertion site of T-DNA (*serf1*; AHHA04) in the coding region (gray box) of *SERF1*. Arrowheads (F and R) and arrows (F^T and R^T) represent positions of gene-specific primers and primers used for detection of the mutant allele. Closed arrowheads (F' and R') represent positions of qRT-PCR primers used for *SERF1* expression analysis.

(C) Validation of established *SERF1* knockdown (KD; black bars; T2 generation), *Ubi*:*SERF1* overexpression (OE; white bars; T0 generation), and *35S*:*SERF1-CFP* constitutive overexpression (COE; gray bars; T0 generation) lines by qRT-PCR analysis on roots. Data represent means ± SE from three independent biological replicates.

RESULTS

Identification of *SERF1*, a Salt-Responsive ERF Gene of the DREB Subfamily

To identify transcriptional regulators involved in the initial response to salt stress in rice, we tested the expression of TF genes in rice roots (cv Nipponbare) during the first 24 h of salt stress (100 mM NaCl). One of the genes identified and selected for characterization is *SALT-RESPONSIVE ERF1* (*SERF1*). *SERF1* expression is induced within 10 min of salt stress and reaches maximal expression after 60 min of treatment (Figure 1A). To evaluate the contribution of *SERF1* to salinity tolerance, we followed a reverse genetics approach. A homozygous T-DNA knockout line, *serf1*, with an insertion in the 3′ end of the single exon of *SERF1* was isolated (Figure 1B). The absence of full-length *SERF1* transcript in homozygous *serf1* plants was confirmed by quantitative RT-PCR (qRT-PCR). To validate any effect observed for the *serf1* mutant, we established knockdown plants by introducing a *SERF1*-specific artificial microRNA, of which three

independent transgenic lines (KD 3-1, KD 4-1, and KD 5-1) were selected for subsequent analyses (Figure 1C). Furthermore, *SERF1* overexpression lines were generated in which *SERF1* is either expressed under the control of the maize (*Zea mays*) *UBIQUITIN* (*Ubi*) promoter or expressed as a fusion protein with cyan fluorescent protein (SERF1-CFP) under control of the cauliflower mosaic virus (CaMV) 35S promoter.

The rice genome encodes 15 group II ERF genes of the DREB subfamily, which can be subdivided into three classes. *SERF1* belongs to group IIc ERFs, which lack both the EAR motif and CMII-3 motif found in members of the groups IIa and IIb (Nakano et al., 2006). Screening the genome of several plant species using Phytozome (Goodstein et al., 2012) revealed that rice, *Arabidopsis*, but also sorghum (*Sorghum bicolor*), brachypodium (*Brachypodium distachyon*), and maize encode each two class IIc ERF genes. The corresponding proteins share a highly conserved AP2 DNA binding domain (see Supplemental Figure 1 online). Furthermore, the C terminus of SERF1 bears two conserved predicted helical structures (H_1 and H_2), of which the latter is only found in monocots. Although the *Arabidopsis* class IIc ERF genes are uncharacterized, it is worth to note that At1g22810 is induced by salt stress in roots (Kilian et al., 2007).

SERF1 Is Induced by H_2O_2 Treatment and Is Expressed in Vascular Tissues

Salinity stress in plants induces both ABA-independent and ABA-dependent signaling pathways together with a rapid induction of osmotic stress (Munns and Tester, 2008). Therefore, we tested the expressional response of *SERF1* in wild-type roots and leaves upon H_2O_2, ABA, or mannitol application (Figure 2A). Application of ABA or mannitol did not affect the expression of *SERF1*. By contrast, as observed for salt stress, H_2O_2 treatment caused an upregulation of *SERF1* within 30 min exclusively in roots, albeit an induction was also observed after 3 h of treatment. Rice plants expressing a β-*glucuronidase* (*GUS*) reporter gene fused to a 1-kb promoter of *SERF1* exhibited GUS activity in the vascular cylinder of the root and the main and commissural veins of leaves (Figure 2B).

Although SERF1 does not contain a known nuclear localization signal, stable transformation of rice plants with a construct encoding a CFP-tagged version of SERF1 revealed nuclear localization of SERF1 in leaf epidermal cells (Figure 2C).

SERF1 Is a Positive Regulator of Short-Term Salt Stress Tolerance

A typical response to salt stress is the closure of stomata, which contributes to water conservation. Thus, the extent to which plants are able to cope with osmotic stress is reflected by their adaptation in leaf transpiration (Sirault et al., 2009). One parameter that characterizes stomatal aperture and, thus, transpiration is leaf temperature. Therefore, measuring leaf temperature by noninvasive infrared thermography allows indirect detection of stomatal conductance (SC) upon stress application (Merlot et al., 2002). Here, we used infrared thermography to quantify leaf temperature of 15-d-old *serf1*, *SERF1* knockdown, and overexpression plants during the initial phase of salt stress.

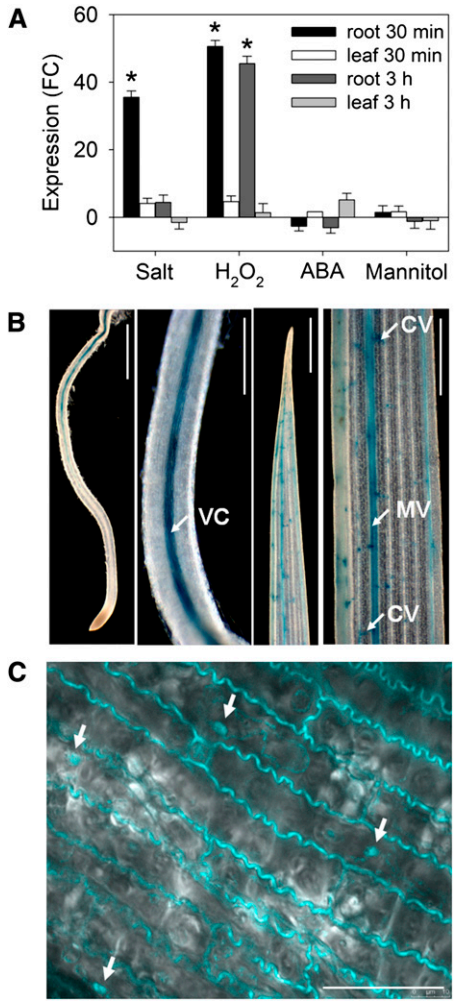

Figure 2. *SERF1* Is Specifically Induced by Salt Stress and H_2O_2 Treatment and Is Expressed in the Vascular Tissues of Roots and Leaves.

(A) Expression of *SERF1* (fold change) in wild-type roots and leaves after exposure to salt stress (100 mM NaCl), ABA (5 μM), mannitol (100 mM), or H_2O_2 (5 mM) for 30 min or 3 h relative to mock-treated control plants. Data are means ± SE of three independent biological replicates, and an asterisk indicates a significant difference ($P \leq 0.05$) from mock-treated roots. FC, fold change.

(B) Staining of mock-treated *SERF1*:*GUS* plants revealed GUS activity (blue) in the vascular cylinder (VC) of roots, main veins (MV), and commissural veins (CV) of leaves. Bars from left to right: 2 mm, 500 μm, 2 mm, and 500 μm.

(C) Nuclear (white arrows) and cytoplasmic localization of SERF1-CFP in rice leaf epidermal cells. Bar = 25 μm.

After application of salt (200 mM NaCl), the leaf temperature increased in all lines. However, from 15 min onwards, *serf1* and the *SERF1* knockdown lines KD 4-1 and KD 5-1 exhibited higher leaf temperature compared with control lines (see Supplemental Figures 2A and 2C online). This finding indicates that loss or knockdown of *SERF1* decreases the tolerance to osmotic stress induced by salt treatment. By contrast, *SERF1* overexpression lines showed lower leaf temperatures after 25 min of salt stress

compared with the empty vector (EV) line (see Supplemental Figure 2D online). Leaf temperature of mock-treated *serf1* plants did not differ from the wild type (see Supplemental Figure 2B online); likewise, *SERF1* knockdown and overexpression plants and their respective controls showed similar leaf temperatures under control conditions.

SERF1 Is a Positive Regulator of Long-Term Salt Stress Tolerance

To evaluate the physiological consequence of *SERF1* expression upon long-term salt stress, 2-week-old plants were exposed to 100 mM NaCl for 7 d. Both *serf1* and KD 4-1 plants accumulated significantly less shoot fresh weight (FW) than wild-type and EV plants (Figure 3A). Furthermore, a significantly decreased relative dry weight (DW) was observed in *serf1* plants (Figure 3B). By contrast, *SERF1* overexpression plants were less impaired in relative shoot growth upon salt stress compared with EV lines. OE 27-1 and OE 14-1 maintained a shoot weight of 82 and 77% of mock-treated plants, respectively, whereas for EV lines, a reduction to 58% of the shoot FW of mock-treated plants was observed (Figure 3C). Furthermore, *SERF1* overexpression plants had 92 and 94% of the shoot DW of unstressed plants, whereas EV plants showed a significantly stronger reduced shoot DW (Figure 3D).

An important aspect of salt tolerance is the avoidance of Na^+ accumulation. Three-week-old hydroponically grown *serf1* and KD 4-1 plants were subjected to 50 mM NaCl for 7 d. Subsequently, roots and leaves were harvested separately at day 0 (no stress) and days 1, 3, 5, and 7 of salt stress. In leaves of *serf1* and the wild type, an increase in Na^+, K^+, and Cl^- content was detected (Figure 3E). Remarkably, at day 5 of salt stress, *serf1* accumulated significantly more Na^+, K^+, and Cl^- than the wild type. Similar to *serf1*, leaves of KD 4-1 contained more Na^+ and Cl^- at day 5 of salt stress than EV plants (Figure 3F). Na^+ and Cl^- content increased continuously under salt stress in all plant lines tested. However, at day 5, *serf1* roots exhibited a significantly increased Na^+ content compared with the wild type. Also, KD 4-1 roots displayed higher Na^+ and Cl^- levels at days 5 and 7. In contrast with Na^+, levels of K^+ declined in the roots of all plant lines tested during salt stress.

The ability to maintain a low Na^+/K^+ ratio contributes to salt tolerance in plants (Zhu, 2003; Conde et al., 2011). There was an increasing Na^+/K^+ ratio detectable for roots and leaves of both *serf1* and the wild type under salt stress. However, at day 5, *serf1* leaves showed a significantly higher Na^+/K^+ ratio than did wild-type leaves (Figure 3E). Moreover, the Na^+/K^+ ratio was significantly higher in KD 4-1 leaves at day 5 of salt stress (Figure 3F).

The accumulation of Na^+ in leaves damages the photosynthetic apparatus (Munns and Tester, 2008). We examined the transpiration rate (TR), SC, and CO_2 assimilation rate (CAR) of the youngest fully expanded leaf of 3-week-old hydroponically grown *serf1* and KD 4-1 plants exposed to 50 mM NaCl for 7 d (see Supplemental Figure 3 online). During the stress period, SC, TR, and CAR declined continuously in *serf1* and wild-type plants. We observed a significantly stronger decline of TR at days 6 and 7 for *serf1* (23 and 18%) compared with the wild type (57 and 36%). Furthermore, at day 7, the wild type maintained 42% of the SC under control conditions, whereas *serf1* exhibited a significantly stronger reduction (22%). A similar observation was made for CAR at these time points (13 and −5% in *serf1* versus 46 and 29% in wild-type plants). Consistent with this, KD 4-1 plants were more strongly affected in TR after 7 d and more strongly affected in SC than EV plants after 6 and 7 d of salt stress, respectively (see Supplemental Figure 3 online).

Overexpression of *SERF1* Increases Oxidative Stress Tolerance

The induction of *SERF1* by H_2O_2 caused us to assess whether SERF1 affects the tolerance to oxidative stress. To this end, leaves were treated for 36 h either with the herbicide methyl viologen (MV), which causes the production of superoxide, or with H_2O_2. Both MV and H_2O_2 treatment resulted in a significantly reduced content of chlorophyll *a* and/or *b* of *serf1* leaves compared with the wild type (see Supplemental Figure 4A online). Also, decreased expression of *SERF1* in knockdown lines resulted in a stronger reduction of chlorophyll *a* after MV and H_2O_2 treatment compared with the EV line (see Supplemental Figure 4B online). By contrast, leaves of plants overexpressing *SERF1* showed higher levels of chlorophyll after either MV or H_2O_2 treatment compared with EV leaves (see Supplemental Figure 4C online). Thus, SERF1 is a positive regulator of oxidative stress tolerance.

Because H_2O_2 levels increase upon salt stress (Hong et al., 2009), we examined the redox homeostasis in roots of *serf1* and the *SERF1* knockdown line. We found no difference in pyridine nucleotide content under control or salt stress conditions (see Supplemental Figures 4D and 4G online). In both wild-type and *serf1* roots, a decrease in $NADP^+$ and NADPH levels was observed upon salt stress. NADP(H) levels determine the sizes and redox states of GSH and ascorbate pools (Takahara et al., 2010). Total GSH levels in the wild type and *serf1* were similar under control conditions (see Supplemental Figures 4E and 4H online). However, in *serf1* and KD 4-1, the amount of reduced GSH was significantly lower. Upon salt stress, the pool of reduced GSH was similar to the wild type, but the total GSH pool decreased significantly in the *serf1* mutant. A similar trend was observed for the knockdown lines of *SERF1*. Measurement of ascorbate levels revealed an opposite trend. Untreated roots of *serf1* and *SERF1* knockdown lines had significantly more reduced ascorbate than the respective controls (see Supplemental Figures 4F and 4I online). Moreover, after salt stress, the total pool of ascorbate increased significantly in *serf1* compared with the wild type.

We performed an H_2O_2-specific histochemical analysis of salt-treated roots and leaves (see Supplemental Figures 4J and 4K online). No difference in 3,3-diaminobenzidine staining intensity was observed between mock-treated *serf1* and wild-type roots. Upon exposure to salt stress for 30 min (100 mM NaCl), an increased staining was observed in roots of both *serf1* and the wild type. By contrast, leaves of both genotypes did not produce more H_2O_2 under short-term salt stress. Still, mock-treated leaves of *serf1* plants showed a slightly stronger staining intensity than the wild type.

Establishment of a Marker Gene Set for the Initial Response to Salt Stress

Mechanisms to cope with salinity involve efficient stress sensing and signaling, cell detoxification systems, compatible solute and

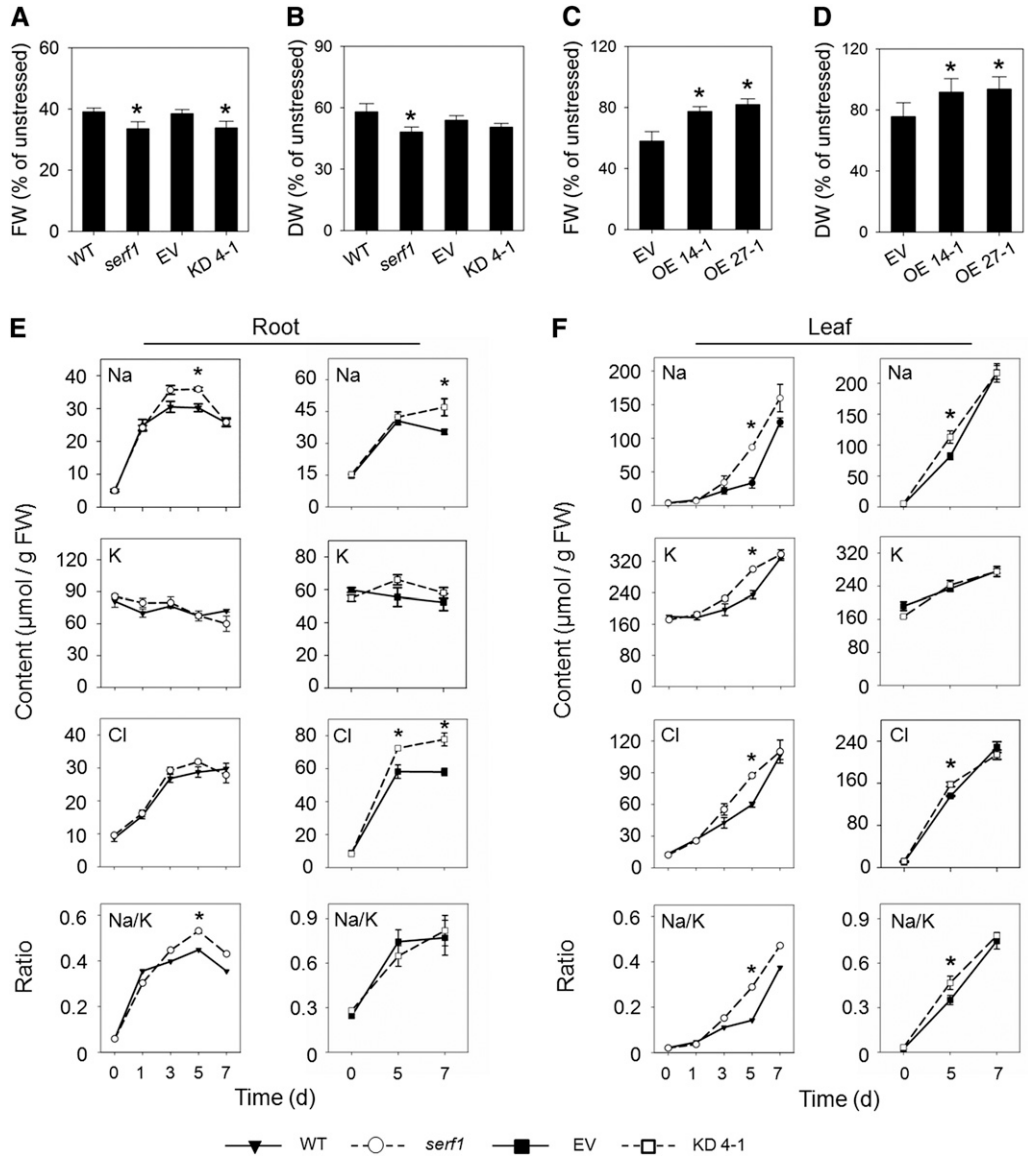

Figure 3. Effect of SERF1 on Biomass Reduction and Ion Accumulation under Long-Term Salt Stress.

(A) to **(D)** Growth inhibition of shoots of 3-week-old plants after 7 d of salinity stress (100 mM NaCl). Relative shoot FW **(A)** and DW **(B)** of salt-stressed wild type (WT), *serf1*, EV, and *SERF1* knockdown (KD 4-1) plants compared with mock-treated plants. Relative shoot FW **(C)** and DW **(D)** of salt-stressed EV and *SERF1* overexpression (OE 14-1 and OE 27-1) plants compared with mock-treated plants. Data in **(A)** to **(D)** represent means ± SD from five independent biological replicates (six plants each), and an asterisk indicates a significant difference in relative growth inhibition between *serf1*, *SERF1* knockdown (KD 4-1), *SERF1* overexpression lines (OE 14-1 and OE 27-1), and their respective controls ($P \leq 0.05$).

(E) and **(F)** Ion content in root **(E)** and leaf tissue **(F)** of 4-week-old wild type, *serf1*, EV, and KD 4-1 plants exposed to salt stress (50 mM NaCl) for 7 d. Day 0 represents the control. Shown are the values for Na^+, K^+, and Cl^- together with the evolution of the Na^+/K^+ ratio over time. Data represent means ± SE from three independent biological replicates, and an asterisk indicates a significant difference ($P \leq 0.05$) to stressed wild-type and EV plants, respectively.

osmoprotectant accumulation, and a vital rearrangement of solute transport and compartmentalization (Conde et al., 2011). At the transcript level, this implies an altered expression of genes involved in MAPK signaling, calcineurin B-like/calcineurin B-like–interacting protein kinase (CBL/CIPK) pathways, and ion transport. Based on literature and homology with other species, we selected rice genes with a potential role in salt stress tolerance for which we established a qRT-PCR expression analysis platform.

Of the 373 initially selected genes, 190 were found to be differentially expressed during the first 24 h of salt stress in roots (see Supplemental Table 1 online). A comparison of the expression profiles during the four time points tested (5 min, 30

min, 3 h, and 24 h) revealed that the majority of the genes (104) were differentially expressed after 24 h of salt stress (see Supplemental Figures 5A and 5B online). On the other hand, two genes (*MAP3K19* and *CIPK24*/*SOS2*) were differentially expressed at all four time points. Genes encoding MAPK-dependent and calcium-dependent signaling components responded strongly during the early phase of salt stress, whereas aquaporins, ion transporters, and channels were mainly differentially expressed after 24 h of salt stress. To exploit the identified salt-responsive marker genes for the characterization of *SERF1*, we selected a subset of 70 genes mainly responding within the first 3 h of salt stress (see Supplemental Figure 5C and Supplemental Table 2 online).

Before testing the expression of these genes in salt-stressed roots of the different plant lines, we first analyzed their response to H_2O_2, ABA, and mannitol (see Supplemental Table 2 online). Forty-two of the 70 selected genes were differentially expressed during the first 3 h of salt stress. Nineteen genes responded similarly to H_2O_2 or salt, of which the majority encoded MAPK and calcium signaling components. On the other hand, the expression of 18 genes overlapped with the response to ABA, including ion channels and transporters. For mannitol, we found 11 responsive genes; however, they were distributed evenly among the functional classes.

SERF1 Affects Genes Related to Sodium Ion Exclusion and Compartmentalization in Roots

Sodium toxicity is in part caused by the impairment of potassium homeostasis. Thus, ion transporters play a key role in salt stress tolerance (Bartels and Sunkar, 2005). In wild-type plants, a decrease in expression of the K^+ channel encoding genes *AKT2/3* and *SKOR* (Os04g36740) was observed during salt stress but not in *serf1* or *SERF1* knockdown lines (see Supplemental Figure 6A online), whereas overexpression lines showed reduced expression levels of *AKT2/3* under control conditions (see Supplemental Table 3 online). On the other hand, the ABA-responsive *HKT8* gene was downregulated in all lines during salt stress (see Supplemental Figure 6B online). Interestingly, genes of the *HAK* family were differentially expressed in the wild type but not in *serf1*. Furthermore, their salt-triggered response could be mimicked by both ABA and H_2O_2 treatments. *HAK* genes were partially impaired in their response in *SERF1* knockdown lines, but their response in *SERF1* overexpression lines was similar to control lines.

Vacuolar sequestration of Na^+ lowers its concentration in the cytoplasm and thereby contributes to osmotic adjustment to maintain water absorption from saline solutions (Silva and Gerós, 2009). In wild-type plants, *VHA-C* and *OVP4* were upregulated during salt stress, a response not observed in *serf1* plants (see Supplemental Figure 6C online). Furthermore, the ATPase-encoding genes *ACA7* and *AHA1* showed a lack of response in roots of *serf1* and *SERF1* knockdown lines and were found to be H_2O_2 responsive (see Supplemental Tables 2 and 3 online).

Although aquaporin genes responded mainly after 24 h of salt stress in the wild type, their expression in *serf1* was affected within 3 h of salt stress (see Supplemental Figure 6D online). In the wild type, only *NIP1-1* was induced under salt stress, while both *NIP1-1* and *TIP4-2* were induced in *serf1* plants. Moreover, expression of the plasma membrane–localized aquaporins *PIP1-3*, *PIP2-1*, *PIP2-3*, and *PIP2-4* was significantly downregulated in *serf1* plants. Consistent with this, KD 5-1 plants showed a stronger response of aquaporin genes (see Supplemental Table 3 online). In *SERF1* overexpression plants, *PIP* gene expression was unaffected during short-term salt stress. The expression of *PIPs* was found to be repressed upon mannitol treatment (see Supplemental Figure 6D online), suggesting a change of osmotic homeostasis in *serf1* during salt stress.

SERF1 Is Required for the Expression of H_2O_2-Responsive Signaling Genes

Among the selected salt-responsive genes encoding MAPK cascade components, nine (*MAPK5*, *MAPK8*, *MAPK15*, *MAP2K6*, *MAP3K4*, *MAP3K6*, *MAP3K15*, *MAP3K18*, and *MAP3K19*) were induced in wild-type roots after 30 min and/or 3 h of salt stress (Figure 4A). By contrast, only three genes (*MAP3K6*, *MAP3K15*, and *MAP3K18*) were induced in stressed *serf1* roots, and their response was attenuated compared with the wild type. Consistently, *MAPK5*, *MAPK15*, *MAP3K4*, *MAP3K6*, *MAP3K12*, and *MAP3K19* also showed an attenuated response in *SERF1* knockdown lines upon salt stress (see Supplemental Table 3 online). By contrast, in *SERF1* overexpression plants, *MAPK5* and *MAP3K23* were upregulated under control conditions. Moreover, increased expression of *MAPK5*, *MAPK8*, *MAPK9*, *MAP2K6*, *MAP3K6*, *MAP3K15*, *MAP3K18*, and *MAP3K19* compared with EV plants was observed after short-term salt stress (see Supplemental Table 3 online). Remarkably, of the six MAPK signaling genes that no longer respond in *serf1* under salt stress, *MAPK5*, *MAPK8*, *MAPK15*, *MAP2K6*, and *MAP3K19* were H_2O_2 inducible (Figure 4A), while short-term ABA or mannitol treatment only marginally affected the expression of these genes.

Calcium acts as an important second messenger in the signal transduction of many abiotic stress responses (Conde et al., 2011). Of the four *CPK* genes tested, only the H_2O_2-responsive *CPK4* gene showed an attenuated response in *serf1* plants under salt stress (see Supplemental Figure 7 online). A weaker response of *CPK4* was also observed in the KD 4-1 line, while in *SERF1* overexpression plants, a similar response to the wild type was seen (see Supplemental Table 3 online). Likewise, *CBL8* and *CBL10* did not respond in stressed *serf1* and *SERF1* knockdown lines, but their response was not affected by *SERF1* overexpression. *CBL10* showed an increased expression in wild-type roots, whereas *CBL8* was downregulated under salt stress, overlapping with the response of these genes to H_2O_2 and ABA. Furthermore, *CIPK6*, *CIPK18*, and *CIPK22* were differentially expressed in the wild type but not in *serf1* (see Supplemental Figure 7 online). Also in KD 4-1 and KD 5-1, *CIPK6* and *CIPK18* did not respond after 30 min of salt stress. Still, overexpression of *SERF1* did not alter the response of these genes. *CIPK6*, *CIPK18*, and *CIPK22* were also differentially expressed after H_2O_2 application (see Supplemental Table 2 online). In *serf1* roots, downregulation of *CIPK4* under salt stress similar to wild-type roots was observed. Although the loss of *SERF1* impaired the expression of several calcium-related

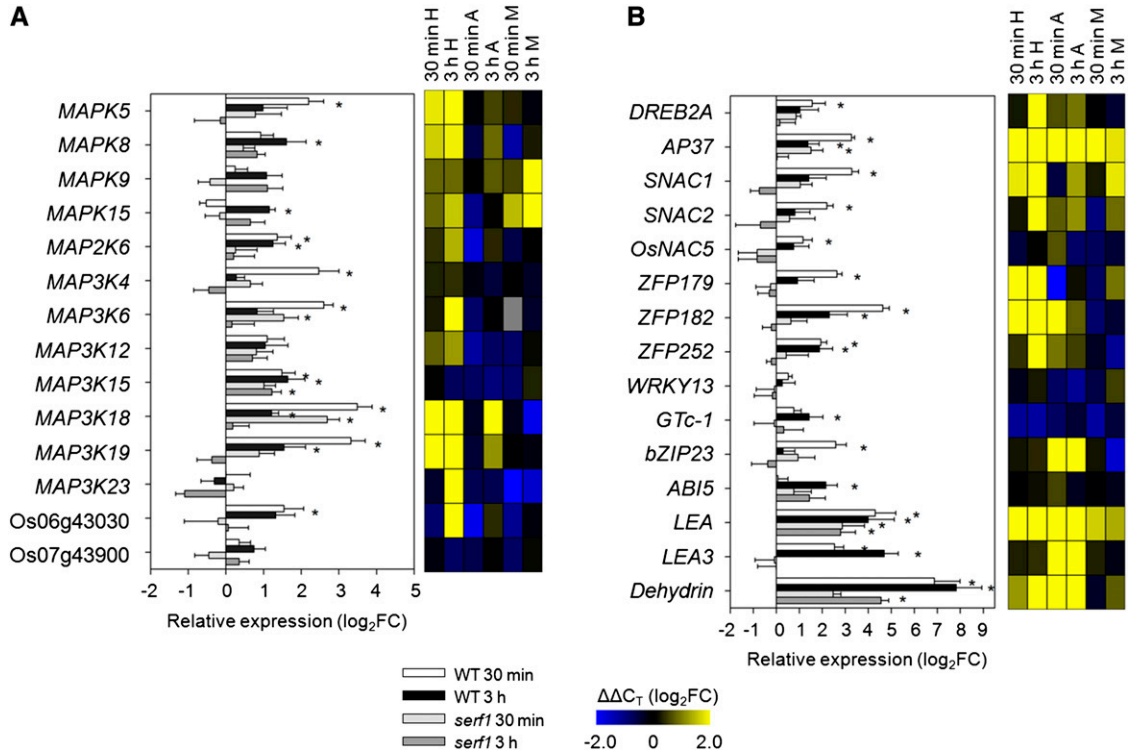

Figure 4. SERF1 Affects the Expression of H_2O_2-Responsive MAPK and TF Genes.

Transcript levels of MAPK cascade genes **(A)** and TF genes **(B)** were measured in roots of wild-type and *serf1* plants subjected to salt stress (100 mM NaCl) for 30 min or 3 h; expression values are normalized to *ACTIN*. Data represent mean $\Delta\Delta C_T \pm$ SE from three independent biological replicates, and an asterisk indicates a significant difference between stressed and mock-treated plants ($P \leq 0.05$) of the same genotype. The heat map presents the response of each gene to 5 mM H_2O_2 (H), 5 μM ABA (A), or 100 mM mannitol (M) after 30 min or 3 h of treatment. Values are given as $\log_2$FC relative to mock-treated wild-type roots; $n = 3$. Os06g43030 and Os07g43900 code for protein kinases. FC, fold change; WT, the wild type.

genes, there was no effect or only a weak effect on the expression of these genes by overexpression of *SERF1*.

SERF1 Is Required for the Induction of Salt Tolerance–Mediating TF Genes

Currently, several TF genes are known to promote salt tolerance when overexpressed in rice. *DREB2A* and *AP37* represent positive regulators of salt tolerance (Oh et al., 2009; Mallikarjuna et al., 2011), both of which were induced in stressed wild-type roots (Figure 4B). By contrast, *DREB2A* was not responsive, and *AP37* showed an attenuated response in *serf1* and *SERF1* knockdown lines upon salt stress (Figure 4B; see Supplemental Table 4 online). In addition to salt stress, both TF genes were H_2O_2 inducible. The transcript levels of the zinc-finger TF genes *ZFP179*, *ZFP182*, and *ZFP252* (Huang et al., 2007; Xu et al., 2008; Sun et al., 2010) were enhanced in wild-type roots after 30 min of salt stress. However, no significant induction was observed in roots of *serf1* and *SERF1* knockdown lines. Furthermore, three NAC TF genes, *SNAC1*, *SNAC2*, and *NAC5* (Hu et al., 2006, 2008; Takasaki et al., 2010), were induced upon salt treatment in the wild type but failed to respond in *serf1* and *SERF1* knockdown lines. Notably, expression of *ZFP179*, *ZFP182*, *ZFP252*, *SNAC1*, and *SNAC2* was enhanced upon H_2O_2 application (Figure 4B).

By contrast, *SERF1* overexpression lines showed enhanced expression of *DREB2A*, *AP37*, *ZFP179*, *ZFP182*, *ZFP252*, *SNAC1*, *SNAC2*, and *NAC5* under control conditions (see Supplemental Table 4 online). Moreover, *ZFP179*, *ZFP182*, and *NAC5* were more strongly induced in *SERF1* overexpression plants than in EV plants after 30 min and/or 3 h of salt stress. In addition, after 3 h of salt stress, *DREB2A* still exhibited enhanced expression levels in *SERF1* overexpression plants, which was not observed in EV plants. Next to that, the induction of three general salt stress marker genes, *LEA3* (Sun et al., 2010), *LEA*, and *Os11g26760*, encoding a dehydrin (Hu et al., 2006), was attenuated in stressed *serf1*, KD 4-1, and KD 5-1 roots (Figure 4B; see Supplemental Table 4 online). By contrast, transcript levels of *LEA3* and *Os11g26760* were elevated in mock-treated or salt-stressed *SERF1* overexpression roots compared with EV.

SERF1 Is a Direct Regulator of *MAP3K6*, *MAPK5*, *DREB2A*, *ZFP179*, and *SERF1*

The 1-kb promoter regions of the salt-responsive genes that we tested were screened for the presence of the drought-responsive element [(A/G)CCGAC], which is typically bound by DREB TFs (Dubouzet et al., 2003). The analysis was restricted to

those genes that were induced by salt stress in the wild type but not *serf1* and showed an induction after H_2O_2 treatment.

Three *MAPK* genes, *MAPK5*, *MAPK8*, and *MAPK15*, and two *MAP3K* genes, *MAP3K6* and *MAP3K19*, fulfilling the above criteria contain at least one copy of the DREB-specific *cis*-element in their promoters (see Supplemental Table 5 online). In addition to *MAPK5*, which contains two DREB-specific motifs, we selected *MAP3K6* for binding studies, as it has been proposed to act as an important integrator of abiotic stress signaling in rice (Jung et al., 2010) and contains a single GCCGAC motif in its promoter (Figure 5A). In addition, the TF genes *DREB2A* and *ZFP179* were selected for binding assays (see Supplemental Table 5 online). Furthermore, *SERF1* itself was selected as it contains a GCCGAC motif at position −40 relative to the transcriptional start site (Figure 5A).

To monitor binding of SERF1 to its targets, an electrophoretic mobility shift assay (EMSA) was performed (Figure 5B). Incubation with two different probes derived from the *MAPK5* promoter with SERF1 resulted in a band shift, indicating that SERF1 binds both DREB motifs in vitro. In addition, we demonstrated binding of SERF1 to probes based on the promoters of *DREB2A*, *MAP3K6*, *ZFP179*, and *SERF1* covering the DREB-specific *cis*-elements at positions (bp) −656, −814, −898, and −40, respectively (Figures 5A to 5C). Competition with unlabeled probes indicated that SERF1 binds specifically to all tested sequences in vitro.

The binding of SERF1 to the promoters of *MAPK5*, *DREB2A*, *MAP3K6*, *ZFP179*, and *SERF1* in vivo was demonstrated by chromatin immunoprecipitation coupled to quantitative PCR (ChIP-qPCR) using *35S:SERF1-CFP* plants (Figure 5D). We observed a 15- and 25-fold enrichment with primers spanning the DREB-specific *cis*-elements at positions −50 and −282 within the *MAPK5* promoter, respectively. Likewise, the use of primers specific for promoter fragments from *MAP3K6*, *DREB2A*, and *SERF1* resulted in an 11-, 58-, and 18-fold enrichment, respectively. Finally, a 650-fold enrichment was observed when using primers spanning the *ZFP179*-specific promoter fragment compared with IgG reactions.

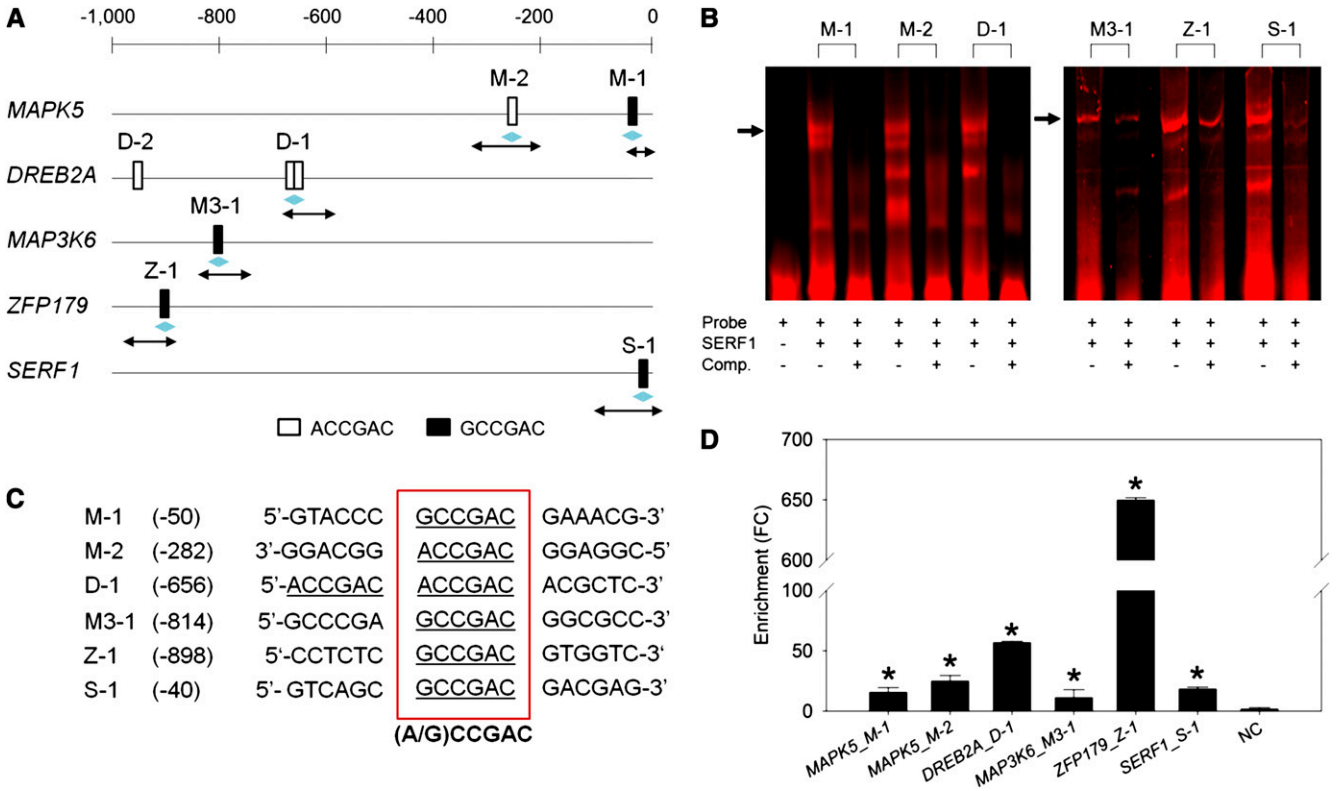

Figure 5. SERF1 Binds to a DREB-Specific *Cis*-Element Present in the Promoters of *MAP3K6*, *MAPK5*, *DREB2A*, *ZFP179*, and *SERF1*.

(A) Position of the DREB binding site 'ACCGAC' (white box) and 'GCCGAC' (black box) in the promoters of putative direct targets of SERF1. Positions of probes used for EMSA (light blue arrows) and ChIP-qPCR–based binding assay (black arrows) are shown below each gene.

(B) EMSA performed with probes specific to *MAPK5* (M-1 and M-2), *DREB2A* (D-1), *MAP3K6* (M3-1), *ZFP179* (Z-1), and *SERF1* (S-1). Binding of SERF1 causes a band shift (black arrow). Upon addition of unlabeled probe (competitor, 100×), the intensity of the shifted band fades. The first lane on the left contains only the labeled probe M-1.

(C) Consensus sequence of the SERF1 binding site (red box).

(D) ChIP-qPCR–based in vivo binding assay with promoter fragments spanning the SERF1 binding site; $n = 3$. Data represent mean values ± SE. As a negative control (NC), a *ZFP179*-specific promoter fragment ~2.1 kb upstream of the transcriptional start site was tested. An asterisk indicates a significant difference ($P \leq 0.05$) to the IgG negative control according to Student's *t* test. FC, fold change.

Because the negative control reaction, in which primers were targeted at amplifying a fragment ~2.1 kb upstream of the SERF1 binding site in the promoter of *ZFP179*, did not show any enrichment, we concluded that the observed enrichments were genuine.

Phosphorylation of SERF1 Increases Its Ability to Activate Transcription of Target Genes

One of the two SERF1 homologs in *Arabidopsis* (encoded by At1g71520) is a potential MAPK phosphorylation target (Popescu et al., 2009), suggesting that SERF1 might represent a target of a rice MAPK cascade. MAPKs phosphorylate a Ser or Thr residue that is followed by a Pro residue (Nakagami et al., 2005). Five Ser residues and one Thr residue are conserved among SERF1 and its homologs (see Supplemental Figure 1 online). Of these, only the Ser residue at position 105 (Ser-105) fulfills the criteria for a MAPK target site (Cohen, 1997).

To test the relevance of a phosphorylated Ser-105 for transcriptional activation of *DREB2A*, *ZFP179*, *MAPK5*, and *SERF1*, we performed a *trans*-activation assay in rice protoplasts using (1) the full-length wild-type *SERF1* open reading frame driven by the CaMV 35S promoter (*SERF1*^{S105}), (2) a SERF1 construct that mimics constitutive phosphorylation by replacing Ser-105 by an Asp residue (*SERF1*^{D105}), or (3) a SERF1 that cannot be phosphorylated due to the substitution of Ser-105 by an Ala residue (*SERF1*^{A105}; Figures 6A to 6D). Cotransformation of the 1-kb promoter regions of *MAPK5*, *DREB2A*, and *SERF1* fused to the firefly luciferase gene (*LUC*) with the *SERF1* construct mimicking phosphorylation (*SERF1*^{D105}) resulted in an approximately twofold higher luminescence signal compared with the Ala-substituted *SERF1* construct (*SERF1*^{A105}; Figures 6A, 6B, and 6D), suggesting a contribution of Ser-105 to the ability of SERF1 to activate its targets. Among the promoter constructs, *DREB2A*:*LUC* and *MAPK5*:*LUC* showed the strongest induction by SERF1^{D105} (>10-fold).

Moreover, no significant activation of *ZFP179*:*LUC* by SERF1^{S105} and SERF1^{A105} was observed, while addition of SERF1^{D105} resulted in a twofold induction. This indicates that phosphorylation of Ser-105 might be mandatory for the activation of *ZFP179* by SERF1 (Figure 6C). For all the tested promoters, except *DREB2A*, the intensity of the luminescence signal induced by the unmodified SERF1^{S105} was between that found for SERF1^{D105} and SERF1^{A105}, suggesting a partial in vivo phosphorylation of SERF1^{S105} by MAPKs present in rice protoplasts. Both the wild-type SERF^{S105} protein and the modified form SERF1^{D105} were nuclear localized when transiently expressed in rice protoplasts (Figure 6E), indicating that phosphorylation does not affect localization of SERF1.

SERF1 Is a Phosphorylation Target of MAPK5

The rice genome contains 17 predicted *MAPK* genes, of which *MAPK5* and *MAPK33* have been reported to play a role in salt stress tolerance (Xiong and Yang, 2003; Lee et al., 2011). *MAPK5* rapidly responds to salt stress in roots and is directly activated by SERF1 (Figures 4 and 5). Genome-wide expression analysis of rice protoplasts transformed with an inducible overexpression construct encoding the constitutively active form of MKK4 (MKK4^{DD}), which was shown to phosphorylate MAPK5, revealed an upregulation of *MAPK5*, *MAP3K6*, *DREB2A*, and *ZFP179* (Kishi-Kaboshi et al., 2010), representing direct targets of SERF1. As the expression patterns of *MAPK5* and *SERF1* are similar during development and under abiotic and biotic stress conditions (Hruz et al., 2008; Jung et al., 2010; this report), we speculated that SERF1 is a phosphorylation target of MAPK5. First, we tested the effect of MAPK5 on SERF1-mediated activation of *MAPK5*, *DREB2A*, *ZFP179*, and *SERF1* (Figures 7A to 7D). Compared with *SERF1*^{S105}, cotransformation of *SERF1*^{S105} and *MAPK5* significantly enhanced the activation of *MAPK5*:*LUC*, *DREB2A*:*LUC*, and *SERF1*:*LUC* reporter constructs (Figures 7A, 7B, and 7D). SERF1^{S105} activated the *ZFP179* promoter only in the presence of MAPK5 (Figure 7C). By contrast, cotransformation of *SERF1*^{A105} with *MAPK5* did not lead to an induction of the four tested promoter-*LUC* fusion constructs compared with *SERF1*^{A105}.

To test whether MAPK5 can phosphorylate SERF1 in vitro, a luminescence-based kinase assay was performed (Figure 7E).

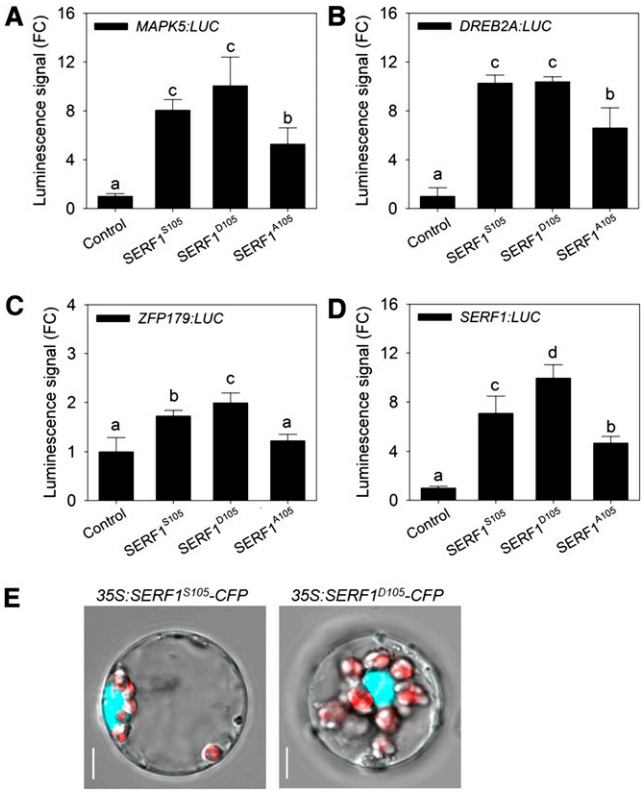

Figure 6. Mutating Ser-105 in SERF1 Alters Its Transcriptional Activity.

(A) to **(D)** Firefly LUC activity (fold change) of *MAPK5*:*LUC* **(A)**, *DREB2A*:*LUC* **(B)**, *ZFP179*:*LUC* **(C)**, and *SERF1*:*LUC* **(D)** in the presence of wild-type SERF1 (SERF1^{S105}), SERF1 mimicking constitutive phosphorylation (SERF1^{D105}), and SERF1 unable to be phosphorylated (SERF1^{A105}) relative to the control (corresponds to basal expression). Values represent means ± SD (n = 3). Different letters (a to d) above bars represent significantly different groups ($P \leq 0.05$) calculated by analysis of variance tests. FC, fold change.

(E) Nuclear localization of SERF1^{S105}-CFP (left panel) and SERF1^{D105}-CFP (right panel) in rice shoot protoplasts. Chloroplasts show red autofluorescence. Bars = 5 μm.

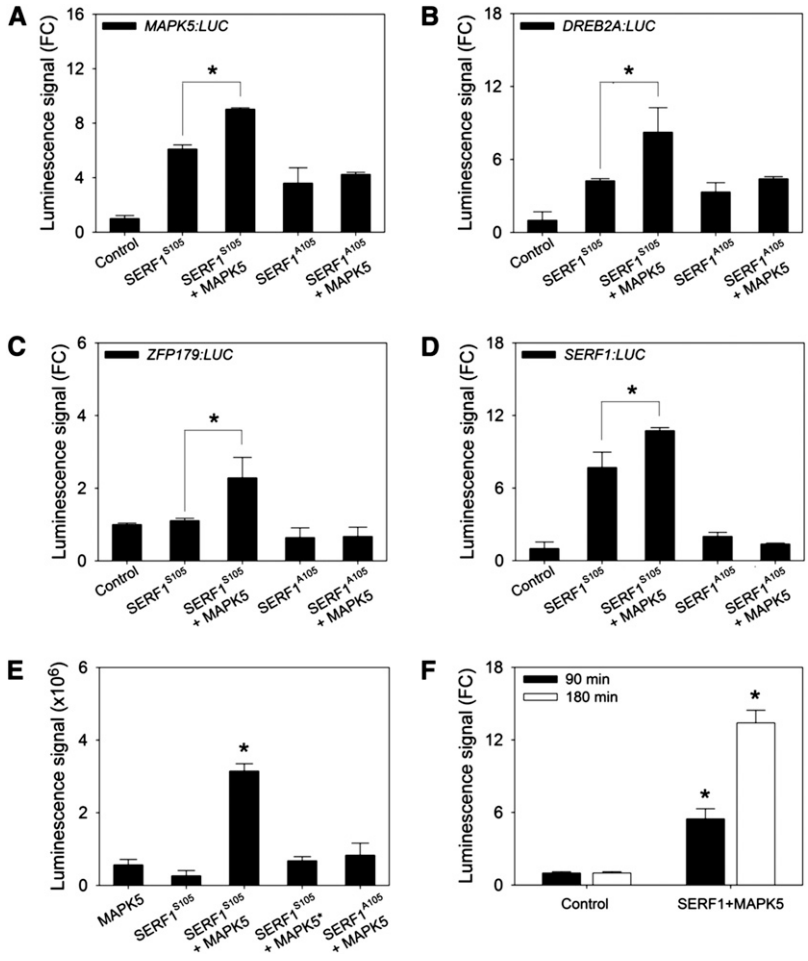

Figure 7. Interaction of SERF1 and MAPK5 Enhances the Transcriptional Activity of SERF1.

(A) to **(D)** LUC activity (fold change [FC]) of *MAPK5*:*LUC* **(A)**, *DREB2A*:*LUC* **(B)**, *ZFP179*:*LUC* **(C)**, and *SERF1*:*LUC* **(D)** in the presence of unmodified SERF1 (SERF1^{S105}) or modified SERF1, which cannot be phosphorylated at position 105 (SERF1^{A105}) with or without MAPK5 relative to the control (corresponds to basal expression). Values represent means ± SD (n = 3). An asterisk indicates a significant difference ($P \leq 0.05$) between the signals caused by SERF1^{S105} alone or SERF1^{S105} in the presence of MAPK5, as calculated by Student's t test.

(E) In vitro kinase assay. The luminescence increased when wild-type SERF1 was incubated with MAPK5. Preheated MAPK5 (10 min 95°C; MAPK5*) or incubation of SERF1^{A105} with MAPK did not enhance LUC activity. ADP consumption is expressed as luminescence signal. Values shown are the means ± SE of four independent reactions. An asterisk indicates a significant difference ($P \leq 0.05$) to control reaction with MAPK5 only according to Student's t test.

(F) Split-luciferase assay with the wild-type *SERF1* CDS fused to the C-terminal part and the *MAPK5* CDS fused to the N-terminal part of *LUC*. Measurements were taken 90 and 180 min after transformation into rice shoot protoplasts. The strength of the luminescence signal is expressed relative to the coexpression of both empty vectors, each containing one-half of the *LUC* gene; n = 3. Data represent means ± SE. An asterisk indicates a significant difference ($P \leq 0.05$) to the control.

With this luminescence assay, the amount of ADP formed after phosphorylation is measured. Incubation of the wild-type SERF1 protein with MAPK5 for 1 h resulted in a significantly increased ADP production, as a more than threefold greater luminescence signal was observed compared with control reactions containing only MAPK5 or SERF1. Consistently, incubation of SERF1 with an inactivated MAPK5 protein (MAPK5* is MAPK5 boiled for 10 min at 95°C) did not increase the luminescence signal. Moreover, phosphorylation of SERF1 by MAPK5 occurs specifically at Ser-105, as incubation of SERF1^{A105} with MAPK5 did not increase the luminescence signal. Finally, we performed a split-luciferase assay to demonstrate the interaction of MAPK5 and SERF1 in vivo. For this assay, the 5′-part of the *LUC* gene was fused downstream of the *MAPK5* open reading frame, while the SERF1 coding sequence (CDS) was cloned in frame with the 3′ part of the *LUC* gene (Figure 7F). When both constructs were transiently expressed in rice protoplasts, a threefold higher luminescence signal relative to empty vector controls was observed 90 min after transformation. The signal further increased after 18 h of incubation.

DISCUSSION

Recently, it has been demonstrated that ROS production by NADPH oxidases is crucial for mediating salt stress tolerance and that exogenous H_2O_2 improves salinity tolerance in *Arabidopsis* (Ma et al., 2012). During the initial phase of salt stress, increased ROS levels might act as an acclimation signal. Here, we present evidence for an H_2O_2-dependent molecular signaling cascade involving the DREB TF SERF1, which coordinates the initial transcriptional response during salinity stress in rice. We propose that SERF1 is required for the propagation of the initial ROS signal to mediate salt tolerance.

SERF1 is a positive regulator of the physiological response to salt stress, as *SERF1* overexpression increased tolerance in terms of a lower leaf temperature and improved shoot biomass accumulation under salt stress (Figures 3C and 3D). By contrast, loss or knockdown of *SERF1* decreased tolerance toward salt stress, as shown by a stronger reduction of shoot biomass (Figures 3A and 3B), a faster accumulation of Na^+ in both roots and shoots (Figures 3E and 3F), and an earlier decline in transpiration and CO_2 assimilation rates. Salinity causes rapid accumulation of H_2O_2 in the vascular cylinder of *Arabidopsis* roots. The root-to-shoot Na^+ transport and, thus, the accumulation of toxic Na^+ levels in shoots under salt stress, is increased in *Arabidopsis* plants lacking *RBOHF*, which encodes a root-localized NADPH oxidase catalyzing ROS production in the root vasculature (Jiang et al., 2012). In rice, it was shown that NaCl treatment causes an increase in H_2O_2 levels in roots within 5 min, and this increase depends on NADPH oxidase activity, as pretreatment with diphenylene iodonium inhibits H_2O_2 accumulation (Hong et al., 2009). *SERF1* expression is specifically induced in roots upon salt stress and H_2O_2 application, but not by ABA or mannitol treatment (Figure 2A). Moreover, GUS activity driven by the *SERF1* promoter is restricted to vascular tissues (Figure 2B). We found that SERF1 modulates the expression of H_2O_2-responsive genes involved in salt stress signaling in roots. As *serf1* roots are capable of accumulating H_2O_2 upon salt stress, it is likely that SERF1 functions in H_2O_2-dependent salt stress signaling rather than H_2O_2 production during salt stress. Therefore, we propose that inadequate H_2O_2 signaling in roots of *serf1* and *SERF1* knockdown lines is responsible for the early accumulation of Na^+ in leaves of those plants.

In addition to functioning as a direct signal molecule, H_2O_2 is necessary for ABA signaling (Kwak et al., 2003). Consistent with the H_2O_2 burst occurring in *serf1* roots upon salt stress, genes related to Na^+ exclusion and compartmentalization, which are responsive to both H_2O_2 and ABA, were only weakly affected by altered expression of *SERF1* during salt stress. As ABA is required for long-term adaptation to salt stress (Maggio et al., 2006), the regulation of these genes by ABA might partially compensate for the lack of the H_2O_2-dependent signaling in *serf1* roots and thereby explain the relatively mild effect of loss or knockdown of *SERF1* on long-term salt stress tolerance.

Induction of TF genes conferring salt stress tolerance (e.g., *DREB2A*, *ZFP179*, *ZFP182*, *ZFP252*, and *SNAC2*) upon salt stress was impaired by the loss of *SERF1* (Figure 4B), while most of them were already induced under control conditions upon *SERF1* overexpression. These results indicate that SERF1 acts upstream of established salt stress regulators. Moreover, we showed that SERF1 directly modulates the transcription of *DREB2A* and *ZFP179* by binding to a DREB-specific *cis*-element present in their promoters (Figure 5). Furthermore, both *DREB2A* and *ZFP179* are H_2O_2 inducible, whereas short-term application of physiologically relevant ABA concentrations did not affect their expression (Figure 4). Interestingly, it was previously reported that rice plants overexpressing *ZFP179* show increased oxidative stress tolerance (Sun et al., 2010), which is in accordance with the decreased tolerance of *serf1* and *SERF1* knockdown plants to oxidative stress, while *SERF1* overexpression lines are more tolerant.

Still, several TF genes acting downstream of SERF1, including *ZFP182* and *SNAC2*, have been reported to be ABA inducible (Hu et al., 2008; Zhang et al., 2012). As H_2O_2 levels increase rapidly upon salt stress (Hong et al., 2009), we propose that the induction of these TF genes is at first regulated by H_2O_2-dependent pathways rather than by signaling pathways mediated by ABA. Similarly, during chilling stress, it has been demonstrated that genes induced by oxidative stress are activated earlier than those responsive to ABA (Yun et al., 2010). It is notable that ABA and ROS signaling pathways affect each other through feed-forward and feedback loops. For example, *ZFP179* is involved in both ABA-dependent and ABA-independent salt

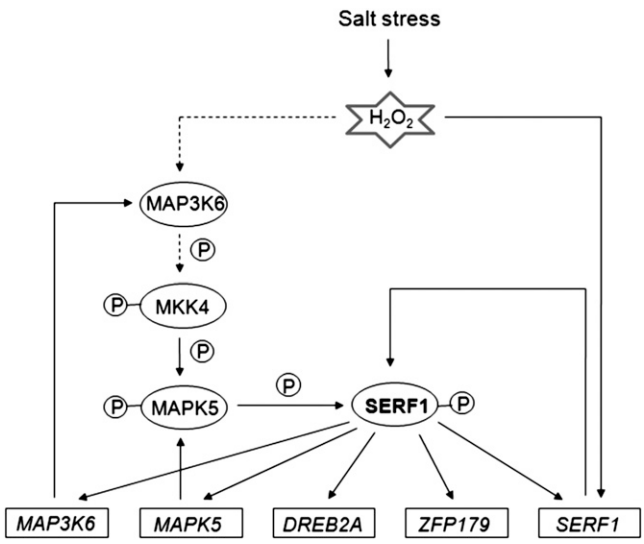

Figure 8. Proposed Role of SERF1 during the Initial Response to Salt Stress.

Salt stress induces the expression of *SERF1*, potentially through H_2O_2 production. At the transcriptional level, SERF1 directly activates the expression of its target genes *MAP3K6*, *MAPK5*, *DREB2A*, and *ZFP179*, and itself. Transcriptional activity of SERF1 is regulated by MAPK5 through phosphorylation of a conserved Ser residue at position 105. The MAPK5-controlled activation of SERF1 allows for the induction of SERF1 target genes within minutes after salt stress. Furthermore, SERF1 functions in a positive feedback loop at the transcriptional level for the salt-responsive MAPK cascade and itself. Solid arrows represent experimentally shown interactions and dotted arrows indicate putative interactions.

stress signaling (Sun et al., 2010). Rice seedlings overexpressing *ZFP179* possess enhanced expression of *DREB2A*, which acts ABA-independently (Dubouzet et al., 2003). Furthermore, overexpression of *bZIP23*, *ZFP179*, and *ZFP252*, genes that did not respond to salt stress in *serf1* roots (Figure 4), increases expression of *LEA3* (Xiang et al., 2008; Xu et al., 2008; Sun et al., 2010). Although *LEA3* expression is ABA dependent, it is affected by the impaired H_2O_2 signaling in *serf1*, probably due to the lack of response(s) of upstream regulator(s).

The relevance of the MAPK signaling pathway for salt tolerance has been well established in *Arabidopsis* (Mizoguchi et al., 1996; Ichimura et al., 2000; Teige et al., 2004; Nakagami et al., 2005), whereas in rice relatively little is known. A MAPK module typically consists of three protein kinases: MAP3K, MAP2K, and MAPK. Upstream signals activate MAP3Ks, which then phosphorylate MAP2Ks. MAP2Ks in turn activate a specific MAPK (Ning et al., 2010). Moreover, MAPK cascades represent well-known ROS-activated signaling networks involved in several abiotic stress pathways (Mittler et al., 2011). Salt stress–induced expression of *MAPK* superfamily genes was severely impaired in *serf1* and *SERF1* knockdown plants, whereas an improved response was observed upon overexpression of *SERF1* (Figure 4A; see Supplemental Table 3 online). Based on expression profiling, six *MAP3K* genes were suggested to play a central role in rice abiotic stress signaling (Jung et al., 2010). Four of these genes, *MAP3K4*, *MAP3K6*, *MAP3K18*, and *MAP3K19*, represent salt-induced *MAP3K* genes, which all showed an attenuated or impaired response to salt stress by the loss or knockdown of *SERF1* and an improved response upon *SERF1* overexpression. Moreover, all four *MAP3K* genes have a SERF1 binding site in their promoters. For *MAP3K6*, we demonstrated that SERF1 recognizes the DREB-specific *cis*-element present in its promoter in vivo (Figure 5D). In addition, SERF1 directly modulates the expression of *MAPK5* (Figure 5), which improves salt tolerance of rice when overexpressed (Xiong and Yang, 2003). Thus, SERF1 represents a transcriptional regulator of MAPK signaling components in rice. Furthermore, MAP3K6 has been proposed, among others, to phosphorylate the salt-responsive MKK4 in rice (Jung et al., 2010).

Remarkably, several TF and MAPK cascade genes acting downstream of SERF1 are activated upon induced expression of $MKK4^{DD}$ in rice protoplasts, including *DREB2A*, *ZFP179*, *MAP3K6*, and *MAPK5* (Kishi-Kaboshi et al., 2010). In addition, it was demonstrated that MAPK5 is phosphorylated by MKK4 (Kishi-Kaboshi et al., 2010), suggesting that SERF1 acts not only upstream but also downstream of a salt-responsive MAPK cascade. Because in wild-type plants, all direct SERF1 targets are induced within 30 min of salt stress (Figure 4), well before the maximum induction of *SERF1* (Figure 1A), it is likely that the early activation of target genes during salt stress does not exclusively occur through the de novo protein synthesis of SERF1 but also by an already present SERF1 protein, which is activated upon salt stress. Phosphorylation of TFs by MAPKs has been shown to modulate transcriptional activity in rice (Cheong et al., 2003; Shen et al., 2012). Indeed, the SERF1 protein contains a Ser residue at position 105 (Ser-105), which is conserved among homologous proteins of both monocots and dicots. Additionally, this Ser residue is followed by a Pro residue, forming the common MAPK target motif (Cohen, 1997). Replacement of Ser-105 by Asp-105, a phosphorylation mimic, enhanced the ability of SERF1 to activate its direct targets in rice protoplasts. On the other hand, substitution by Ala-105, a non-phosphorylatable residue, weakened the induction of *MAPK5*, *DREB2A*, *ZFP179*, and *SERF1* (Figure 6). In the case of *ZFP179*, mimicked phosphorylation of SERF1 was even mandatory for a significant induction. However, substitution of Ser-105 by Asp-105 does not affect the nuclear localization of SERF1.

MAPK5 and MAPK33 have been functionally characterized regarding their contribution to salt stress tolerance in rice. In contrast with MAPK33, which negatively affects the salt stress response (Lee et al., 2011), MAPK5 acts as a positive regulator of salinity tolerance (Xiong and Yang, 2003). Using a split-luciferase assay, we demonstrated that MAPK5 interacts with SERF1 in vivo (Figure 7F). Furthermore, the presence of MAPK5 increased the expression of direct SERF1 targets in rice protoplasts, which is achieved through the phosphorylation of Ser-105, as its replacement by Ala-105 abolished the stimulating effect of MAPK5 (Figure 7). Consistently, MAPK5 was able to phosphorylate in vitro the wild-type form of SERF1 possessing Ser-105, but not the modified form containing Ala-105 (Figure 7). Thus, SERF1 acts as an output of the MAPK cascade that positively feeds back onto the expression of the signaling components. Additionally, we found that SERF1 directly activates its own promoter (Figure 5), thereby establishing a second positive feedback loop in the molecular signaling cascade.

In summary, we discovered an H_2O_2-mediated molecular signaling cascade important for the initial response to salinity in rice (Figure 8). We have shown that SERF1 is a phosphorylation target of a salt-responsive MAPK, thereby promoting the expression of MAPK cascade genes (*MAPK5* and *MAP3K6*), salt tolerance–mediating TF genes (*ZFP179* and *DREB2A*), and itself through direct interaction with the corresponding promoters in planta. In essence, salt stress results in a wave of H_2O_2 production (Mittler et al., 2011) that activates SERF1 through the MAPK pathway. Posttranslational regulation of H_2O_2-dependent *SERF1* expression is consistent with the observation that ROS signals occur rapidly during environmental changes (Hong et al., 2009; Mittler et al., 2011). When key players are present within the cell, a quick initial response is guaranteed. Moreover, nuclear translocation of activated MAPK proteins has been observed during abiotic stress (Ahlfors et al., 2004; Im et al., 2012), keeping MAPK and potential nuclear target TFs separated under control conditions. This first ROS wave is propagated at the transcriptional level through SERF1. However, as the transcriptional activity of SERF1 is modulated by phosphorylation, only a persistent salt stress signal will further boost the expression of target genes. In such a scenario, a transient stress can be sensed rapidly, and activation of stress genes is stopped before full activation of the acclimation program.

METHODS

Plant Material and Growth Conditions

Seeds of wild-type rice plants (*Oryza sativa* cv Nipponbare) and transgenic rice plants were placed on hydroponic boxes with full-strength Yoshida medium (Yoshida et al., 1976) using Styrofoam adaptors. Plants were grown for 3 or 4 weeks at (day/night) 26/22°C, 75/70% relative humidity,

with a daylength of 12 h and a light intensity of 700 $\mu mol \cdot m^{-2} \cdot s^{-1}$. T2 seeds of *SERF1* knockdown and EV lines and T1 seeds of *SERF1* overexpression lines were selected on 40 mg/L hygromycin. Leaves and roots were harvested separately.

Salt, Mannitol, ABA, and H_2O_2 Treatments

All salt, ABA, mannitol, and H_2O_2 treatments were replicated in at least three independent biological experiments. Two-week-old or 3-week-old hydroponically grown plants were treated with either 50 or 100 mM NaCl by adding the appropriate amount of a 5 M NaCl solution to the 10 liters of growth medium. Furthermore, 4-week-old hydroponically grown plants were treated with 100 mM NaCl, 100 mM mannitol, 5 μM ABA, or 5 mM H_2O_2. After each treatment, tissue was immediately frozen in liquid nitrogen and stored at −80°C until further use.

Isolation of a T-DNA Insertion Mutant

The rice mutant *serf1* (ssp *japonica* cv Nipponbare) was obtained from the Génoplante Oryza Tag Line collection (T-DNA insert DAH3F06, line AHHA04) (Sallaud et al., 2004). Homozygous T2 plants were confirmed by PCR using primers 5′-AAAACTGATGGCAAATTCGC-3′ and 5′-GTCTGGACCGATGGCTGTGTAGAAG-3′ for mutant allele and primers 5′-GAGTGAGGAGCTCATTGTTTACGA-3′ and 5′-GTGTCCATGATTCCTTGGTTTAGT-3′ for wild-type allele detection, respectively. Seeds of homozygous plants were propagated two times, and T4 seeds were used for analysis.

Constructs and Rice Transformation

For construction of an artificial microRNA specific to *SERF1* to produce knockdown lines, primers were designed using WMD2 (http://wmd2.weigelworld.org) harboring *att*B sites. Subsequently, multistep PCR was performed as described previously (Warthmann et al., 2008). The artificial microRNA construct was cloned into pC5300 OE vector according to Schmidt et al. (2012). For construction of *SERF1* overexpression lines, the full-length CDS of *SERF1* was synthesized and sequence verified by GeneArt. Subsequently, the *SERF1* CDS was either recombined into pIPKb002 (Himmelbach et al., 2007) for generating *Ubi*:*SERF1* plants or cloned in frame at its 3′ end with CFP CDS in the pGHPGWC vector for generating *35S*:*SERF1-CFP* plants (Zhong et al., 2008). *SERF1*:*GUS* plants were generated by recombining a 1-kb promoter sequence immediately upstream of the TSS of *SERF1* into pMDC162 (Curtis and Grossniklaus, 2003) using a two-step cloning strategy involving pENTR/D-TOPO (Invitrogen). Calli of rice (cv Nipponbare) were cocultured with *Agrobacterium tumefaciens* strain EHA105 containing recombinant or EVs according to Sallaud et al. (2003). Oligonucleotide sequences used for cloning are listed in Supplemental Table 6 online.

Subcellular Localization of SERF1

Rice shoot protoplasts were obtained and transformed with the *35S*:*SERF1-CFP* construct according to Zhang et al. (2011). Fluorescence imaging of the protoplasts was performed using a confocal laser scanning microscope (SP5; Leica Microsystems).

Detection of GUS Activity

Roots and leaves of *SERF1*:*GUS* plants were stained overnight in GUS solution according to Jefferson (1987).

RNA Extraction and qRT-PCR

RNA isolation and cDNA synthesis for expression profiling on roots and leaves were performed as described previously (Caldana et al., 2007). Three biological replicates were used for each experiment. qRT-PCR was performed in a 5-μL reaction using Power SYBR Green PCR Master Mix (Applied Biosystems). *ACTIN* (Os03g50885, forward primer 5′-CTCCCCCATGCTATCCTTCG-3′ and reverse primer 5′-TGAATGAGTAACCACGCTCCG-3′) served as the reference gene according to Caldana et al. (2007). Relative transcript abundance was calculated by the comparative cycle threshold (C_T) method (Livak and Schmittgen, 2001). Oligonucleotide sequences for expression profiling of early salt-responsive marker genes were designed with QuantPrime (Arvidsson et al., 2008). Oligonucleotide sequences used for expression profiling of the 373 genes involved in salt stress response and TF genes are listed in Supplemental Tables 7 and 8 online.

EMSA and ChIP-qPCR

To obtain protein for EMSA assays, the *SERF1* CDS was subcloned into the pF3A WG Flexi vector (Promega). For in vitro expression, 3.5 μg of plasmid DNA was added to the TNT SP6 High Yield Wheat Germ Mastermix containing 1 μL FluoroTec Green Lys (Promega). After 2 h of incubation at 30°C, the protein abundance was analyzed by SDS-PAGE and subsequent fluorescent detection using a Typhoon Scanner (GE Healthcare). For gel-shift assays, Cy5-labeled probes were generated based on a 35- to 40-bp sequence from the target gene promoters containing the SERF1 binding site (see Supplemental Table 9 online). Complementary reverse oligonucleotides and a set of unlabeled forward oligonucleotides were obtained. Probes were annealed in a PCR machine by mixing forward and reverse oligonucleotides in equimolar ratios and slowly cooling them from 95 to 30°C.

Probes were diluted to a final concentration of 500 fmol/μL and kept in amber tubes until use. Binding reactions were performed using the LightShift chemiluminescent assay kit (Pierce) according to the manufacturer's instructions. Protein-DNA complexes were separated on a 5% native polyacrylamide gel after which the Cy5 signal was imaged using a Typhoon Scanner (GE Healthcare).

35S:*SERF1-CFP* transgenic lines used for ChIP-qPCR were grown on soil as described by Degenkolbe et al. (2009). ChIP analysis with the EpiQuik Plant ChIP kit (Epigentek Group) was essentially performed as previously described (Lai et al., 2012). Leaf tissue was cross-linked with 1% (v/v) formaldehyde for 10 min. For the immunopurification of the SERF1-CFP:DNA complexes, a mouse anti-GFP antibody (Roche Applied Science) was used. For each qPCR reaction, 1 μL of the purified DNA was used. Enrichments were calculated by first normalizing the obtained C_T values with the input C_T and subsequent computation of $\Delta\Delta C_T$ (C_T(IgG) – C_T(anti-GFP)). Primers used are listed in Supplemental Table 10 online and were designed with the Primer3 software tool (Rozen and Skaletsky, 2000).

Trans-Activation Assay

Rice shoot protoplasts were isolated and transformed according to Zhang et al. (2011). Constructs for *trans*-activation assays were generated by amplifying 1-kb upstream promoter sequences of *DREB2A*, *ZFP179*, *SERF1*, and *MAPK5* by PCR (see Supplemental Table 6 online). After cloning into pENTR/D-TOPO (Invitrogen), the promoter sequences were recombined with the p2GWL7,0 vector (Licausi et al., 2011) to place them upstream of the firefly *LUC* gene. The wild-type and mutated *SERF1* CDSs were cloned from pENTR/D-TOPO into the vector p2GW7,0 (Karimi et al., 2002) containing the CaMV 35S promoter. Protoplasts were cotransformed with the recombinant p2GWL7,0 vectors, normalization vector containing *35S*:*RLUC* (Licausi et al., 2011), and recombinant p2GW7,0 vectors using 5 μg of each plasmid. Dual luciferase reporter assays (Promega) were performed as previously described (Licausi et al., 2011). Luminescence was measured using a GloMax 20/20 luminometer (Promega).

Cell-Free Kinase Assay

To demonstrate that SERF1 is a phosphorylation target of MAPK5, we produced both proteins using the TNT SP6 high-yield wheat germ extract system combined with an ADP-Glo kinase assay (Promega) as described previously (Tadokoro et al., 2010; Nemoto et al., 2011) with several modifications. The CDSs of *SERF1*^{S105}, *MAPK5*, and *SERF1*^{A105} were cloned into pF3A WG (BYDV) Flexi vector (Promega) using the *Pme*I and *Sgf*I restriction sites. For in vitro protein synthesis, 3 μg plasmid was added to 30 μL wheat germ extract containing 0.5 μL FluoroTect Green$_{Lys}$ (Promega) to validate successful protein synthesis. For each ADP-Glo kinase assay, 2 μL of crude protein extract was used. Kinase reactions were performed in triplicate and incubated for 60 min at room temperature in kinase buffer A (40 mM Tris, pH 7.5, 20 mM $MgCl_2$, and 0.1 mg/mL BSA). For normalization, control reactions incubated for 0 min were run for each sample. Reactions were stopped by adding ADP-Glo reagent (Promega) and incubated for 60 min at room temperature. Finally, kinase detection reagent (Promega) was added, and after 60 min of incubation, luminescence was measured with a GloMax 20/20 luminometer (Promega). The ATP used during the reaction was determined as change in luminescence signal by subtracting the signal intensity from the 60 min incubated samples with those incubated for 0 min.

Split-Luciferase Assay

Split-luciferase luminescence assays were performed as described previously (Fujikawa and Kato, 2007) with minor modifications. The *SERF1* and *MAPK5* CDSs cloned into pENTR/D-TOPO (Invitrogen) were subcloned into the expression vectors D7 and pDuExAn6, respectively (Fujikawa and Kato, 2007). Sequences of oligonucleotides used for cloning of *SERF1* and *MAPK5* are listed in Supplemental Table 6 online. Subsequently, plasmids were transformed into rice shoot protoplasts according to Zhang et al. (2011). After transformation and incubation, the protoplasts were lysed and the renilla luciferase (RLUC) signal was measured with the Dual-Luciferase reporter assay kit using a GloMax 20/20 luminometer (Promega). For each plasmid combination, four independent transformations were performed.

Infrared Thermography

Spatially resolved leaf temperature profiles were obtained as described previously (Lisso et al., 2011). In brief, a thermal imaging camera (PIRuc 180; InfraTec) recorded leaf temperature profiles at preset time intervals. Images were saved online by application of the IRBIS-3 thermography software (InfraTec). The experiment was performed in a custom-designed phytochamber to exclude environmentally induced temperature fluctuations and keep thermal noise as low as possible. During kinetic thermography recordings, the experimental plants were exposed to actinic photon flux densities of 300 $\mu mol \cdot m^{-2} \cdot s^{-1}$ provided by two fiber optics light sources (Novaflex; WPI). Averaged leaf temperature values were calculated in defined areas of interest.

Determination of Redox Metabolites and H_2O_2 Detection

Extraction and quantification of pyridine nucleotides were performed by an enzyme cycling assay according to the method described by Obata et al. (2011). GSH was derivatized with monobromobimane and analyzed by reverse-phase HPLC as described by Kreft et al. (2003), except that the polyvinylpolypyrrolidone was omitted from the extraction solution and that the extracts were treated just after extraction without freezing. Ascorbate contents were determined by a spectrophotometric assay described by Stevens et al. (2006) using a part of the plant extract obtained for GSH analysis. H_2O_2 detection in roots was performed at room temperature in the dark with a 1 mg/mL 3,3-diaminobenzidine solution for 24 h.

Oxidative Stress Tolerance Analysis

Oxidative stress tolerance tests were performed as previously described (Fukao et al., 2011) with the following modifications; 5 μM MV was used and the incubation time was extended to 36 h. Pigment content was spectrophotometrically quantified according to Wellburn (1994).

Ion Content Measurement

Plant material (50 mg) was homogenized and dissolved in 500 μL ultrapure water and heated (70°C) for 30 min. After centrifugation at 21,000*g* for 10 min, the supernatant was filtered using an Ultrafree MC 5000 MC NMWL filter unit (Millipore). Anions were analyzed by high-performance anion-exchange chromatography with conductivity detection facilitated by a Dionex ICS-3000 system. Ions were eluted using a reagent-free (RFIC) potassium hydroxide eluent cartridge (Dionex). Anions were separated on an IonPac AS11 column (Dionex) applying a hydroxide gradient (flow: 0.25 mL/min; 0 min: 12 mM KOH; 5 to 8 min, 44 mM KOH; 10 min: 52 mM KOH; 12 to 17 min: 12 mM KOH). Cations were analyzed by high-performance cation-exchange chromatography with conductivity detection facilitated by a Dionex ICS-3000 system. Cations were separated on an IonPac CS12A column (Dionex) and eluted by an isocratic application of 20 mM methanosulfonic acid.

Gas Exchange Measurements

Gas exchange measurements were performed as described previously (von Caemmerer and Farquhar, 1981; Muschak et al., 1999) using a portable infrared gas exchange measuring system (HCM-1000; Walz). Gas exchange measurements were performed on fully expanded upermost leaves of 10 plants per genotype to estimate SC, transpiration, and CO_2 assimilation.

Accession Numbers

Sequence data from this article can be found in the GenBank/EMBL database or the Michigan State University Rice Genome Annotation Project database (http://rice.plantbiology.msu.edu; Ouyang et al., 2007) using the Michigan State University accession numbers: *SERF1* (Os05g34730, GenBank JQ246414), *DREB2A* (Os01g07120), *ZFP179* (Os01g62190), *MAPK5* (Os03g17700), and *ACTIN* (Os03g50885). *serf1* (ssp *japonica* cv Nipponbare) was obtained from the Génoplante Oryza Tag Line collection (T-DNA insert DAH3F06, line AHHA04).

Supplemental Data

The following materials are available in the online version of this article.

Supplemental Figure 1. SERF1 Protein Sequence.

Supplemental Figure 2. Overexpression of *SERF1* Decreases Leaf Temperature under Short-Term Salt Stress.

Supplemental Figure 3. Loss and Knockdown of *SERF1* Lead to Salt Sensitivity by Rapid Decline of Photosynthesis under Salt Stress.

Supplemental Figure 4. SERF1 Affects Oxidative Stress Tolerance and Redox Homeostasis.

Supplemental Figure 5. Identification of Early Salt-Responsive Marker Genes.

Supplemental Figure 6. SERF1 Affects Osmotic Homeostasis and Ion Detoxification/Compartmentalization under Short-Term Salt Stress in Roots.

Supplemental Figure 7. SERF1 Affects the Expression of Genes Involved in Calcium-Dependent Signaling.

Supplemental Table 1. Early Salt-Responsive Genes Identified.

Supplemental Table 2. Response of Selected Salt-Responsive Genes to H_2O_2, ABA, and Mannitol Treatment.

Supplemental Table 3. Expression of Selected Salt-Responsive Genes in *SERF1* Knockdown and Overexpression Lines.

Supplemental Table 4. Expression of Key Transcription Factor Genes in *SERF1* Knockdown and Overexpression Plants.

Supplemental Table 5. Putative Direct SERF1 Target Genes Identified.

Supplemental Table 6. Sequences of Oligonucleotides Used for Cloning Constructs.

Supplemental Table 7. Sequences of Oligonucleotides Used for Expression Profiling of 373 Genes Involved in the Salt Stress Response.

Supplemental Table 8. Sequences of Oligonucleotides Used for Expression Profiling of Transcription Factor Genes with a Known Role in Salt Tolerance.

Supplemental Table 9. Probes Used for EMSA.

Supplemental Table 10. Probes Used for ChIP-qPCR.

ACKNOWLEDGMENTS

This work was in part conducted within the European Reseacrh Area Network Plant Genomics project 'TRIESTER - Trilateral Initiative for Enhancing Salt Tolerance in Rice' for which funding was provided by the Bundesministerium für Bildung und Forschung (BMBF) in Germany (Grant 0313993A), the Agence Nationale de la Recherche in France (Grant ANR-06-ERAPG-005-01), and Ministerio de Educación y Ciencia (Grant GEN2006-27794-C4-1-E) in Spain. Part of this work was conducted on the Rice Functional Genomics platform, Montpellier, France, funded by Agropolis Foundation. R.S. thanks the FAZIT Stiftung for providing a PhD fellowship. We thank Eugenia Maximova and Daan Weits for microscopy work, Heidemarie Heldt for performing the thermography measurements, and Slobodan Ruzicic and Janine Turner for technical assistance.

AUTHOR CONTRIBUTIONS

R.S., J.H.M.S., and B.M.-R. designed the research. R.S. and J.H.M.S. conducted the research and analyzed the data. H.-M.H. and R.H. performed ion measurements. T.O. and A.R.F. performed redox homeostasis measurements. J.F. contributed thermography and gas exchange measurements as analytical tools. D.M. and E.G. did the rice transformations. B.S.S. contributed analytical tools. R.S., J.H.M.S., and B.M.-R. wrote the article.

Received April 25, 2013; revised May 13, 2013; accepted June 2, 2013; published June 25, 2013.

REFERENCES

Ahlfors, R., Macioszek, V., Rudd, J., Brosché, M., Schlichting, R., Scheel, D., and Kangasjärvi, J. (2004). Stress hormone-independent activation and nuclear translocation of mitogen-activated protein kinases in *Arabidopsis thaliana* during ozone exposure. Plant J. **40:** 512–522.

Arvidsson, S., Kwasniewski, M., Riaño-Pachón, D.M., and Mueller-Roeber, B. (2008). QuantPrime—A flexible tool for reliable high-throughput primer design for quantitative PCR. BMC Bioinformatics **9:** 465.

Bartels, D., and Sunkar, R. (2005). Drought and salt tolerance in plants. Crit. Rev. Plant Sci. **24:** 23–58.

Bienert, G.P., Schjoerring, J.K., and Jahn, T.P. (2006). Membrane transport of hydrogen peroxide. Biochim. Biophys. Acta **1758:** 994–1003.

Boudsocq, M., and Laurière, C. (2005). Osmotic signaling in plants: Multiple pathways mediated by emerging kinase families. Plant Physiol. **138:** 1185–1194.

Caldana, C., Scheible, W.R., Mueller-Roeber, B., and Ruzicic, S. (2007). A quantitative RT-PCR platform for high-throughput expression profiling of 2500 rice transcription factors. Plant Methods **3:** 7.

Cheng, C., Yun, K.Y., Ressom, H.W., Mohanty, B., Bajic, V.B., Jia, Y., Yun, S.J., and de los Reyes, B.G. (2007). An early response regulatory cluster induced by low temperature and hydrogen peroxide in seedlings of chilling-tolerant japonica rice. BMC Genomics **8:** 175.

Cheong, Y.H., et al. (2003). BWMK1, a rice mitogen-activated protein kinase, locates in the nucleus and mediates pathogenesis-related gene expression by activation of a transcription factor. Plant Physiol. **132:** 1961–1972.

Cohen, P. (1997). The search for physiological substrates of MAP and SAP kinases in mammalian cells. Trends Cell Biol. **7:** 353–361.

Conde, A., Chaves, M.M., and Gerós, H. (2011). Membrane transport, sensing and signaling in plant adaptation to environmental stress. Plant Cell Physiol. **52:** 1583–1602.

Curtis, M.D., and Grossniklaus, U. (2003). A Gateway cloning vector set for high-throughput functional analysis of genes in planta. Plant Physiol. **133:** 462–469.

Davletova, S., Schlauch, K., Coutu, J., and Mittler, R. (2005). The zinc-finger protein Zat12 plays a central role in reactive oxygen and abiotic stress signaling in *Arabidopsis*. Plant Physiol. **139:** 847–856.

Degenkolbe, T., Do, P.T., Zuther, E., Repsilber, D., Walther, D., Hincha, D.K., and Köhl, K.I. (2009). Expression profiling of rice cultivars differing in their tolerance to long-term drought stress. Plant Mol. Biol. **69:** 133–153.

Dubouzet, J.G., Sakuma, Y., Ito, Y., Kasuga, M., Dubouzet, E.G., Miura, S., Seki, M., Shinozaki, K., and Yamaguchi-Shinozaki, K. (2003). *OsDREB* genes in rice, *Oryza sativa* L., encode transcription activators that function in drought-, high-salt- and cold-responsive gene expression. Plant J. **33:** 751–763.

Fujikawa, Y., and Kato, N. (2007). Split luciferase complementation assay to study protein-protein interactions in *Arabidopsis* protoplasts. Plant J. **52:** 185–195.

Fukao, T., Yeung, E., and Bailey-Serres, J. (2011). The submergence tolerance regulator SUB1A mediates crosstalk between submergence and drought tolerance in rice. Plant Cell **23:** 412–427.

Goodstein, D.M., Shu, S., Howson, R., Neupane, R., Hayes, R.D., Fazo, J., Mitros, T., Dirks, W., Hellsten, U., Putnam, N., and Rokhsar, D.S. (2012). Phytozome: A comparative platform for green plant genomics. Nucleic Acids Res. **40** (Database issue)**:** D1178–D1186.

Himmelbach, A., Zierold, U., Hensel, G., Riechen, J., Douchkov, D., Schweizer, P., and Kumlehn, J. (2007). A set of modular binary vectors for transformation of cereals. Plant Physiol. **145:** 1192–1200.

Hong, C.Y., Chao, Y.Y., Yang, M.Y., Cheng, S.Y., Cho, S.C., and Kao, C.H. (2009). NaCl-induced expression of glutathione reductase in roots of rice (*Oryza sativa* L.) seedlings is mediated through hydrogen peroxide but not abscisic acid. Plant Soil **320:** 103–115.

Hruz, T., Laule, O., Szabo, G., Wessendorp, F., Bleuler, S., Oertle, L., Widmayer, P., Gruissem, W., and Zimmermann, P. (2008). Genevestigator v3: A reference expression database for the meta-analysis of transcriptomes. Adv. Bioinforma. **2008:** 420747.

Hu, H., Dai, M., Yao, J., Xiao, B., Li, X., Zhang, Q., and Xiong, L. (2006). Overexpressing a NAM, ATAF, and CUC (NAC) transcription factor enhances drought resistance and salt tolerance in rice. Proc. Natl. Acad. Sci. USA **103:** 12987–12992.

Hu, H., You, J., Fang, Y., Zhu, X., Qi, Z., and Xiong, L. (2008). Characterization of transcription factor gene *SNAC2* conferring cold and salt tolerance in rice. Plant Mol. Biol. **67:** 169–181.

Huang, J., Yang, X., Wang, M.M., Tang, H.J., Ding, L.Y., Shen, Y., and Zhang, H.S. (2007). A novel rice C2H2-type zinc finger protein lacking DLN-box/EAR-motif plays a role in salt tolerance. Biochim. Biophys. Acta **1769:** 220–227.

Ichimura, K., Mizoguchi, T., Yoshida, R., Yuasa, T., and Shinozaki, K. (2000). Various abiotic stresses rapidly activate *Arabidopsis* MAP kinases ATMPK4 and ATMPK6. Plant J. **24:** 655–665.

Im, J.H., Lee, H., Kim, J., Kim, H.B., and An, C.S. (2012). Soybean MAPK, GMK1 is dually regulated by phosphatidic acid and hydrogen peroxide and translocated to nucleus during salt stress. Mol. Cells **34:** 271–278.

Jefferson, R.A. (1987). Assaying chimeric genes in plants: The GUS gene fusion system. Plant Mol. Biol. Rep. **5:** 387–405.

Jiang, C., Belfield, E.J., Mithani, A., Visscher, A., Ragoussis, J., Mott, R., Smith, J.A., and Harberd, N.P. (2012). ROS-mediated vascular homeostatic control of root-to-shoot soil Na delivery in *Arabidopsis*. EMBO J. **31:** 4359–4370.

Jung, K.H., Cao, P., Seo, Y.S., Dardick, C., and Ronald, P.C. (2010). The Rice Kinase Phylogenomics Database: A guide for systematic analysis of the rice kinase super-family. Trends Plant Sci. **15:** 595–599.

Karimi, M., Inzé, D., and Depicker, A. (2002). GATEWAY vectors for *Agrobacterium*-mediated plant transformation. Trends Plant Sci. **7:** 193–195.

Kilian, J., Whitehead, D., Horak, J., Wanke, D., Weinl, S., Batistic, O., D'Angelo, C., Bornberg-Bauer, E., Kudla, J., and Harter, K. (2007). The AtGenExpress global stress expression data set: Protocols, evaluation and model data analysis of UV-B light, drought and cold stress responses. Plant J. **50:** 347–363.

Kishi-Kaboshi, M., Okada, K., Kurimoto, L., Murakami, S., Umezawa, T., Shibuya, N., Yamane, H., Miyao, A., Takatsuji, H., Takahashi, A., and Hirochika, H. (2010). A rice fungal MAMP-responsive MAPK cascade regulates metabolic flow to antimicrobial metabolite synthesis. Plant J. **63:** 599–612.

Kong, X., Sun, L., Zhou, Y., Zhang, M., Liu, Y., Pan, J., and Li, D. (2011). ZmMKK4 regulates osmotic stress through reactive oxygen species scavenging in transgenic tobacco. Plant Cell Rep. **30:** 2097–2104.

Kreft, O., Hoefgen, R., and Hesse, H. (2003). Functional analysis of cystathionine γ-synthase in genetically engineered potato plants. Plant Physiol. **131:** 1843–1854.

Kwak, J.M., Mori, I.C., Pei, Z.M., Leonhardt, N., Torres, M.A., Dangl, J.L., Bloom, R.E., Bodde, S., Jones, J.D., and Schroeder, J.I. (2003). NADPH oxidase *AtrbohD* and *AtrbohF* genes function in ROS-dependent ABA signaling in *Arabidopsis*. EMBO J. **22:** 2623–2633.

Lai, A.G., Doherty, C.J., Mueller-Roeber, B., Kay, S.A., Schippers, J.H.M., and Dijkwel, P.P. (2012). CIRCADIAN CLOCK-ASSOCIATED 1 regulates ROS homeostasis and oxidative stress responses. Proc. Natl. Acad. Sci. USA **109:** 17129–17134.

Lee, S.K., Kim, B.G., Kwon, T.R., Jeong, M.J., Park, S.R., Lee, J.W., Byun, M.O., Kwon, H.B., Matthews, B.F., Hong, C.B., and Park, S.C. (2011). Overexpression of the mitogen-activated protein kinase gene *OsMAPK33* enhances sensitivity to salt stress in rice (*Oryza sativa* L.). J. Biosci. **36:** 139–151.

Licausi, F., Weits, D.A., Pant, B.D., Scheible, W.R., Geigenberger, P., and van Dongen, J.T. (2011). Hypoxia responsive gene expression is mediated by various subsets of transcription factors and miRNAs that are determined by the actual oxygen availability. New Phytol. **190:** 442–456.

Lisso, J., Schröder, F., Fisahn, J., and Müssig, C. (2011). NFX1-LIKE2 (NFXL2) suppresses abscisic acid accumulation and stomatal closure in *Arabidopsis thaliana*. PLoS ONE **6:** e26982.

Livak, K.J., and Schmittgen, T.D. (2001). Analysis of relative gene expression data using real-time quantitative PCR and the $2^{(-\Delta\Delta\ C(T))}$ method. Methods **25:** 402–408.

Ma, L., Zhang, H., Sun, L., Jiao, Y., Zhang, G., Miao, C., and Hao, F. (2012). NADPH oxidase AtrbohD and AtrbohF function in ROS-dependent regulation of Na^+/K^+homeostasis in *Arabidopsis* under salt stress. J. Exp. Bot. **63:** 305–317.

Maggio, A., Zhu, J.K., Hasegawa, P.M., and Bressan, R.A. (2006). Osmogenetics: Aristotle to *Arabidopsis*. Plant Cell **18:** 1542–1557.

Mallikarjuna, G., Mallikarjuna, K., Reddy, M.K., and Kaul, T. (2011). Expression of OsDREB2A transcription factor confers enhanced dehydration and salt stress tolerance in rice (*Oryza sativa* L.). Biotechnol. Lett. **33:** 1689–1697.

Merlot, S., Mustilli, A.C., Genty, B., North, H., Lefebvre, V., Sotta, B., Vavasseur, A., and Giraudat, J. (2002). Use of infrared thermal imaging to isolate *Arabidopsis* mutants defective in stomatal regulation. Plant J. **30:** 601–609.

Miao, Y., Laun, T., Zimmermann, P., and Zentgraf, U. (2004). Targets of the WRKY53 transcription factor and its role during leaf senescence in *Arabidopsis*. Plant Mol. Biol. **55:** 853–867.

Mittler, R., Vanderauwera, S., Gollery, M., and Van Breusegem, F. (2004). Reactive oxygen gene network of plants. Trends Plant Sci. **9:** 490–498.

Mittler, R., Vanderauwera, S., Suzuki, N., Miller, G., Tognetti, V.B., Vandepoele, K., Gollery, M., Shulaev, V., and Van Breusegem, F. (2011). ROS signaling: The new wave? Trends Plant Sci. **16:** 300–309.

Mizoguchi, T., Irie, K., Hirayama, T., Hayashida, N., Yamaguchi-Shinozaki, K., Matsumoto, K., and Shinozaki, K. (1996). A gene encoding a mitogen-activated protein kinase kinase kinase is induced simultaneously with genes for a mitogen-activated protein kinase and an S6 ribosomal protein kinase by touch, cold, and water stress in *Arabidopsis thaliana*. Proc. Natl. Acad. Sci. USA **93:** 765–769.

Mochida, K., and Shinozaki, K. (2010). Genomics and bioinformatics resources for crop improvement. Plant Cell Physiol. **51:** 497–523.

Munns, R. (2005). Genes and salt tolerance: Bringing them together. New Phytol. **167:** 645–663.

Munns, R., and Tester, M. (2008). Mechanisms of salinity tolerance. Annu. Rev. Plant Biol. **59:** 651–681.

Muschak, M., Willmitzer, L., and Fisahn, J. (1999). Gas-exchange analysis of chloroplastic fructose-1,6-bisphosphatase antisense potatoes at different air humidities and at elevated $CO_{(2)}$. Planta **209:** 104–111.

Nakagami, H., Pitzschke, A., and Hirt, H. (2005). Emerging MAP kinase pathways in plant stress signalling. Trends Plant Sci. **10:** 339–346.

Nakano, T., Suzuki, K., Fujimura, T., and Shinshi, H. (2006). Genome-wide analysis of the *ERF* gene family in *Arabidopsis* and rice. Plant Physiol. **140:** 411–432.

Nemoto, K., Seto, T., Takahashi, H., Nozawa, A., Seki, M., Shinozaki, K., Endo, Y., and Sawasaki, T. (2011). Autophosphorylation profiling of *Arabidopsis* protein kinases using the cell-free system. Phytochemistry **72:** 1136–1144.

Ning, J., Li, X., Hicks, L.M., and Xiong, L. (2010). A Raf-like MAPKKK gene *DSM1* mediates drought resistance through reactive oxygen species scavenging in rice. Plant Physiol. **152:** 876–890.

Nishizawa, A., Yabuta, Y., Yoshida, E., Maruta, T., Yoshimura, K., and Shigeoka, S. (2006). *Arabidopsis* heat shock transcription factor A2 as a key regulator in response to several types of environmental stress. Plant J. **48:** 535–547.

Obata, T., Matthes, A., Koszior, S., Lehmann, M., Araújo, W.L., Bock, R., Sweetlove, L.J., and Fernie, A.R. (2011). Alteration of

mitochondrial protein complexes in relation to metabolic regulation under short-term oxidative stress in *Arabidopsis* seedlings. Phytochemistry **72:** 1081–1091.

Oh, S.J., Kim, Y.S., Kwon, C.W., Park, H.K., Jeong, J.S., and Kim, J.K. (2009). Overexpression of the transcription factor AP37 in rice improves grain yield under drought conditions. Plant Physiol. **150:** 1368–1379.

Ouyang, S., et al. (2007). The TIGR Rice Genome Annotation Resource: Improvements and new features. Nucleic Acids Res. **35** (Database issue)**:** D883–D887.

Pang, C.H., and Wang, B.S. (2008). Oxidative stress and salt tolerance in plants. In Progress in Botany, Vol. 69, U. Lüttge, W. Beyschlag, and J. Murata, eds. (Berlin, Germany: Springer), pp. 231–245.

Popescu, S.C., Popescu, G.V., Bachan, S., Zhang, Z., Gerstein, M., Snyder, M., and Dinesh-Kumar, S.P. (2009). MAPK target networks in *Arabidopsis thaliana* revealed using functional protein microarrays. Genes Dev. **23:** 80–92.

Rozen, S., and Skaletsky, H. (2000). Primer3 on the WWW for general users and for biologist programmers. Methods Mol. Biol. **132:** 365–386.

Sallaud, C., et al. (2004). High throughput T-DNA insertion mutagenesis in rice: A first step towards *in silico* reverse genetics. Plant J. **39:** 450–464.

Sallaud, C., et al. (2003). Highly efficient production and characterization of T-DNA plants for rice (*Oryza sativa* L.) functional genomics. Theor. Appl. Genet. **106:** 1396–1408.

Schippers, J.H.M., Nguyen, H.M., Lu, D., Schmidt, R., and Mueller-Roeber, B. (2012). ROS homeostasis during development: an evolutionary conserved strategy. Cell. Mol. Life Sci. **69:** 3245–3257.

Schmidt, R., Schippers, J.H.M., Welker, A., Mieulet, D., Guiderdoni, E., and Mueller-Roeber, B. (2012). Transcription factor OsHsfC1b regulates salt tolerance and development in *Oryza sativa* ssp. japonica. AoB Plants **2012:** pls011.

Shen, H., Liu, C., Zhang, Y., Meng, X., Zhou, X., Chu, C., and Wang, X. (2012). OsWRKY30 is activated by MAP kinases to confer drought tolerance in rice. Plant Mol. Biol. **80:** 241–253.

Shi, J., Kim, K.N., Ritz, O., Albrecht, V., Gupta, R., Harter, K., Luan, S., and Kudla, J. (1999). Novel protein kinases associated with calcineurin B-like calcium sensors in *Arabidopsis*. Plant Cell **11:** 2393–2405.

Silva, P., and Gerós, H. (2009). Regulation by salt of vacuolar H^+-ATPase and H^+-pyrophosphatase activities and Na^+/H^+ exchange. Plant Signal. Behav. **4:** 718–726.

Sirault, X.R.R., James, R.A., and Furbank, R.T. (2009). A new screening method for osmotic component of salinity tolerance in cereals using infrared thermography. Funct. Plant Biol. **36:** 970–977.

Skopelitis, D.S., Paranychianakis, N.V., Paschalidis, K.A., Pliakonis, E.D., Delis, I.D., Yakoumakis, D.I., Kouvarakis, A., Papadakis, A.K., Stephanou, E.G., and Roubelakis-Angelakis, K.A. (2006). Abiotic stress generates ROS that signal expression of anionic glutamate dehydrogenases to form glutamate for proline synthesis in tobacco and grapevine. Plant Cell **18:** 2767–2781.

Stevens, R., Buret, M., Garchery, C., Carretero, Y., and Causse, M. (2006). Technique for rapid, small-scale analysis of vitamin C levels in fruit and application to a tomato mutant collection. J. Agric. Food Chem. **54:** 6159–6165.

Sun, S.J., Guo, S.Q., Yang, X., Bao, Y.M., Tang, H.J., Sun, H., Huang, J., and Zhang, H.S. (2010). Functional analysis of a novel Cys2/His2-type zinc finger protein involved in salt tolerance in rice. J. Exp. Bot. **61:** 2807–2818.

Tadokoro, D., Takahama, S., Shimizu, K., Hayashi, S., Endo, Y., and Sawasaki, T. (2010). Characterization of a caspase-3-substrate kinome using an N- and C-terminally tagged protein kinase library produced by a cell-free system. Cell Death Dis. **1:** e89.

Takahara, K., Kasajima, I., Takahashi, H., Hashida, S.N., Itami, T., Onodera, H., Toki, S., Yanagisawa, S., Kawai-Yamada, M., and Uchimiya, H. (2010). Metabolome and photochemical analysis of rice plants overexpressing *Arabidopsis* NAD kinase gene. Plant Physiol. **152:** 1863–1873.

Takasaki, H., Maruyama, K., Kidokoro, S., Ito, Y., Fujita, Y., Shinozaki, K., Yamaguchi-Shinozaki, K., and Nakashima, K. (2010). The abiotic stress-responsive NAC-type transcription factor OsNAC5 regulates stress-inducible genes and stress tolerance in rice. Mol. Genet. Genomics **284:** 173–183.

Teige, M., Scheikl, E., Eulgem, T., Dóczi, R., Ichimura, K., Shinozaki, K., Dangl, J.L., and Hirt, H. (2004). The MKK2 pathway mediates cold and salt stress signaling in *Arabidopsis*. Mol. Cell **15:** 141–152.

von Caemmerer, S., and Farquhar, G.D. (1981). Some relationships between the biochemistry of photosynthesis and the gas exchange of leaves. Planta **153:** 376–387.

Warthmann, N., Chen, H., Ossowski, S., Weigel, D., and Hervé, P. (2008). Highly specific gene silencing by artificial miRNAs in rice. PLoS One **3:** e1829.

Wellburn, A.R. (1994). The spectral determination of chlorophyll-a and chlorophyll-b, as well as total carotenoids, using various solvents with spectrophotometers of different resolution. J. Plant Physiol. **144:** 307–313.

Xiang, Y., Tang, N., Du, H., Ye, H., and Xiong, L. (2008). Characterization of OsbZIP23 as a key player of the basic leucine zipper transcription factor family for conferring abscisic acid sensitivity and salinity and drought tolerance in rice. Plant Physiol. **148:** 1938–1952.

Xiong, L., and Yang, Y. (2003). Disease resistance and abiotic stress tolerance in rice are inversely modulated by an abscisic acid-inducible mitogen-activated protein kinase. Plant Cell **15:** 745–759.

Xu, D.Q., Huang, J., Guo, S.Q., Yang, X., Bao, Y.M., Tang, H.J., and Zhang, H.S. (2008). Overexpression of a TFIIIA-type zinc finger protein gene *ZFP252* enhances drought and salt tolerance in rice (*Oryza sativa* L.). FEBS Lett. **582:** 1037–1043.

Yang, Y., Xu, S., An, L., and Chen, N. (2007). NADPH oxidase-dependent hydrogen peroxide production, induced by salinity stress, may be involved in the regulation of total calcium in roots of wheat. J. Plant Physiol. **164:** 1429–1435.

Yoshida, S., Forno, D.A., Cock, S.H., and Gomez, K.A. (1976). Routine procedure for growing rice plants in culture solution. In Laboratory Manual for Physiological Studies of Rice, 3rd Ed. S. Yoshida, ed. (Manila, the Philippines: IRRI), pp 61–66.

Yu, L., Nie, J., Cao, C., Jin, Y., Yan, M., Wang, F., Liu, J., Xiao, Y., Liang, Y., and Zhang, W. (2010). Phosphatidic acid mediates salt stress response by regulation of MPK6 in *Arabidopsis thaliana*. New Phytol. **188:** 762–773.

Yun, K.Y., Park, M.R., Mohanty, B., Herath, V., Xu, F., Mauleon, R., Wijaya, E., Bajic, V.B., Bruskiewich, R., and de Los Reyes, B.G. (2010). Transcriptional regulatory network triggered by oxidative signals configures the early response mechanisms of japonica rice to chilling stress. BMC Plant Biol. **10:** 16.

Zhang, H., Ni, L., Liu, Y., Wang, Y., Zhang, A., Tan, M., and Jiang, M. (2012). The C2H2-type zinc finger protein ZFP182 is involved in abscisic acid-induced antioxidant defense in rice. J. Integr. Plant Biol. **54:** 500–510.

Zhang, Y., Su, J., Duan, S., Ao, Y., Dai, J., Liu, J., Wang, P., Li, Y., Liu, B., Feng, D., Wang, J., and Wang, H. (2011). A highly efficient rice green tissue protoplast system for transient gene expression and studying light/chloroplast-related processes. Plant Methods **7:** 30.

Zhong, S., Lin, Z., Fray, R.G., and Grierson, D. (2008). Improved plant transformation vectors for fluorescent protein tagging. Transgenic Res. **17:** 985–989.

Zhu, J.K. (2003). Regulation of ion homeostasis under salt stress. Curr. Opin. Plant Biol. **6:** 441–445.

SALT-RESPONSIVE ERF1 Regulates Reactive Oxygen Species–Dependent Signaling during the Initial Response to Salt Stress in Rice
Romy Schmidt, Delphine Mieulet, Hans-Michael Hubberten, Toshihiro Obata, Rainer Hoefgen, Alisdair R. Fernie, Joachim Fisahn, Blanca San Segundo, Emmanuel Guiderdoni, Jos H.M. Schippers and Bernd Mueller-Roeber
Plant Cell 2013;25;2115-2131; originally published online June 25, 2013;
DOI 10.1105/tpc.113.113068

This information is current as of July 12, 2015

Supplemental Data	**http://www.plantcell.org/content/suppl/2013/06/17/tpc.113.113068.DC1.html**
References	This article cites 87 articles, 27 of which can be accessed free at: http://www.plantcell.org/content/25/6/2115.full.html#ref-list-1
Permissions	https://www.copyright.com/ccc/openurl.do?sid=pd_hw1532298X&issn=1532298X&WT.mc_id=pd_hw1532298X
eTOCs	Sign up for eTOCs at: http://www.plantcell.org/cgi/alerts/ctmain
CiteTrack Alerts	Sign up for CiteTrack Alerts at: http://www.plantcell.org/cgi/alerts/ctmain
Subscription Information	Subscription Information for *The Plant Cell* and *Plant Physiology* is available at: http://www.aspb.org/publications/subscriptions.cfm

© American Society of Plant Biologists
ADVANCING THE SCIENCE OF PLANT BIOLOGY